



**SATELLITE COMMUNICATIONS IN THE V AND W BANDS
TROPOSPHERIC EFFECTS**

THESIS

Bertus A. Shelters, V, Second Lieutenant, USAF

AFIT-ENG-18-M-060

**DEPARTMENT OF THE AIR FORCE
AIR UNIVERSITY**

AIR FORCE INSTITUTE OF TECHNOLOGY

Wright-Patterson Air Force Base, Ohio

DISTRIBUTION STATEMENT A.

APPROVED FOR PUBLIC RELEASE; DISTRIBUTION UNLIMITED.

The views expressed in this thesis are those of the author and do not reflect the official policy or position of the United States Air Force, the Department of Defense, or the United States Government.

This material is declared a work of the U.S. Government and is not subject to copyright protection in the United States.

AFIT-ENG-18-M-060

SATELLITE COMMUNICATIONS IN THE V AND W BANDS
TROPOSPHERIC EFFECTS

THESIS

Presented to the Faculty
Department of Electrical and Computer Engineering
Graduate School of Engineering and Management
Air Force Institute of Technology
Air University
Air Education and Training Command
in Partial Fulfillment of the Requirements for the
Degree of Master of Science in Electrical Engineering

Bertus A. Shelters, V, B.S.E.E.

Second Lieutenant, USAF

March 2018

DISTRIBUTION STATEMENT A.
APPROVED FOR PUBLIC RELEASE; DISTRIBUTION UNLIMITED.

SATELLITE COMMUNICATION IN THE V AND W BANDS:
TROPOSPHERIC EFFECTS

Bertus A. Shelters, BS
Second Lieutenant, USAF

Committee Membership:

Dr. A. J. Terzuoli
Chair

Maj J.L. Burley, PhD
Member

Dr. S.T. Fiorino
Member

Col D.F. Fuller, PhD
Member

Dr. S Mudaliar
Member

Maj. O.A. Nava, PhD
Member

Abstract

An investigation into the use of Weather Cubes compiled by the atmospheric characterization package, Laser Environmental Effects Definition and Reference (LEEDR), to develop accurate, long-term attenuation statistics for link-budget analysis is presented. A Weather Cube is a three-dimensional mesh of numerical weather prediction (NWP) data plus LEEDR calculations that allows for the quantification of rain, cloud, aerosol, and molecular effects at any UV to RF wavelength on any path contained within the cube. The development of this methodology is motivated by the potential use of V (40-75 GHz) and W (75-110 GHz) band frequencies for the satellite communication application, as V and W band frequencies incur very significant lower atmospheric attenuation. Total path attenuation probability of exceedance curves are compared against ground based radiometric measurements of slant-path attenuation in the V and W bands, as well as relevant International Telecommunication Union recommendations. The results of this work demonstrate the need for further improvements in this methodology.

To Absent Friends

Acknowledgments

This work could not be possible without the support of the committee, the sponsor, our research team, and the Air Force Institute of Technology Center for Directed Energy (CDE).

Bertus A. Shelters, V

Table of Contents

	Page
Abstract	iv
Dedication	v
Acknowledgments	vi
Table of Contents	vii
List of Figures	x
List of Tables	xii
List of Acronyms	xiii
 I. Introduction	 1
1.1 Introduction	1
1.2 Problem Statement	2
1.3 Justification	3
1.4 Approach and Methodology	3
1.5 Assumptions and Scope	4
1.6 Standards	4
1.7 Research Question	4
1.8 Materials	4
1.9 Other	4
 II. Background	 5
2.1 Chapter Overview	5
2.2 Link-Budget Analysis	5
2.3 V and W Band Satellite Communications (SATCOM)	7
2.4 Historical Millimeter Wave Propagation Studies	9
2.5 Measurement Campaigns in the V and W Band	9
2.6 Modeling Campaigns in the V and W band	11
2.7 Weather Cubes and LEEDR	13

	Page
III. Methodology	15
3.1 Chapter Overview	15
3.2 Attenuation Calculations	15
3.2.1 Molecular Absorption	18
3.2.2 Rain and Cloud Absorption and Scattering	20
3.2.3 Aerosol Absorption and Scattering	21
3.3 Calculation of a Slant Path Attenuation	21
3.4 Weather Cubes	22
3.4.1 Physical Size	24
3.4.2 Weather Placement Algorithm [1]	24
3.4.3 Slant Path Calculations	26
3.5 Long-Term Statistics	32
3.6 International Telecommunication Union Recommendations	33
3.6.1 ITU-R Molecular Absorption	34
3.6.2 ITU-R Cloud Absorption [2]	34
3.6.3 ITU-R Rain Effects	34
3.6.4 Total ITU-R Attenuation	35
3.7 Model Error Figure	35
IV. Results Analysis	37
4.1 Introduction	37
4.2 Trial One	37
4.2.1 Trial One Results	38
4.3 Trial Two	39
4.3.1 Trial Two Results	40
4.4 Trial Three	42
4.4.1 Trial Three Results	43
4.5 Trial Four	44
4.5.1 Trial Four Results	46
4.6 Best and Worst Case Analysis	46
4.7 Full Results Analysis	49
V. Conclusion	57
5.1 Conclusion	57
5.2 Comparison With Other Models	58
5.3 Application and Impact	59
5.4 Future Work	59
5.4.1 Adjustment of Weather Placement Algorithm	59
5.4.2 Verification and Validation	60

	Page
5.4.3 Tropospheric Scintillation	61
Appendix: Attenuation Calculations	62
References	65

List of Figures

Figure	Page
3.1 Stratification of Atmosphere	17
3.2 Weather Cube Block Diagram	23
3.3 Five by Five Weather Cube	25
3.4 Five by Five Cube Plotted on Local Level Coordinate System	26
3.5 Weather fields Placed in a Weather Cube	27
3.6 Slant path geometry	30
3.7 Path Altitude Calculation	31
3.8 ITU-R Derived Comparison Data	36
4.1 Trial One: Exceedance Curve	39
4.2 Calculation of Molecular Extinction	40
4.3 Trial Two: Exceedance Curve	42
4.4 Trail Two: Error Figure	43
4.5 Trial Two: Molecular Model Comparison	44
4.6 Trial Two: Cloud Model Comparison	45
4.7 Trial Two: Rain Model Comparison	46
4.8 Trial Three: Exceedance Curve	47
4.9 Trail Three: Error Figure	48
4.10 Trial Four: Exceedance Curve	49
4.11 Trail Four: Error Figure	50
4.12 Worst Case Attenuation Event	51
4.13 Worst Case Extinction Profile	52
4.14 Least Case Attenuation Event	53
4.15 Least Case Extinction Profile	54

Figure	Page
4.16 Rain and Cloud Error Figures	55
4.17 Attenuation Histogram	56
A.1 Comparison of Attenuation Calculation Methods	64

List of Tables

Table	Page
3.1 Molecular Absorption Species Used in LEEDR	20
3.2 Weather Placement Algorithm Thresholds	28
3.3 Rain Placement Thresholds	29
3.4 ITU-R Recommendations Used in this Work	33
4.1 Overview of Configurations Considered in this Research	38
4.2 Trial Two: Error Figure Statistics	41
4.3 Trial Three: Error Figure Statistics	45
4.4 Trial Four: Error Figure Statistics	47
4.5 Summary of Error Results from Each Trial	50
4.6 Highest Attenuation Values for Each Frequency from Trial Four	55

List of Acronyms

Acronym	Definition
AFRL	Air Force Research Laboratory
SNR	Signal to Noise Ratio
SATCOM	Satellite Communications
VWBF	V and W Band Frequencies
UHF	Ultra High Frequency
NWP	Numerical Weather Prediction
LEEDR	Laser Environmental Effects Definition and Reference
CDE	Air Force Institute of Technology Center for Directed Energy
PMT	Propagation Mitigation Techniques
PSM	Pulse Shape Modulation
NOMADS	NOAA Operational Model Archive and Distribution System
GFS	National Oceanic and Atmospheric Administration Global Forecast System
HITRAN	High-Resolution Transmission Molecular Absorption Database
UTC	Coordinated Universal Time
BER	Bit Error Rate
CCDF	Complementary Cumulative Distribution Function
RF	Radio Frequency
EHF	Extremely High Frequency
GADS	Global Aerosol Data Set
ITU-R	International Telecommunication Union Radiocommunication Sector
ExPERT	Extreme and Percentile Environmental Reference Tables
MPM	Millimeter Wave Propagation Model

Acronym	Definition
ATM PROP	Atmospheric Simulator for Propagation Applications
WRF	Weather Research and Forecasting Model

SATELLITE COMMUNICATIONS IN THE V AND W BANDS

TROPOSPHERIC EFFECTS

I. Introduction

1.1 Introduction

The evolution of communications infrastructure to accommodate the increase in the number of users and data consumed by each user can be accomplished by using higher frequencies. Next generation communication systems will utilize V and W band frequencies (40-115 GHz) to address this increase in demand. While short-distance, terrestrial V and W band frequency links exist, these bands have not been used for Satellite Communications (SATCOM). The use of these frequencies offer several benefits for the strategic SATCOM application. The narrow beam-width potential results in a low probability of detection and interception. Smaller antenna and hardware components would take up less space on a satellite payload [3]. No commercial entities currently use this band for SATCOM, thus large portions of the spectrum are available for this application. Higher frequency signals also have a level of resiliency to ionospheric effects.

V and W band frequencies were not considered for SATCOM in the past because of the significant atmospheric propagation impairments incurred. Compared to the lower Ultra High Frequency (UHF), Ku, and Ka bands used for SATCOM, V and W Band Frequencies (VWBF) are more attenuated by tropospheric extinction. Whereas rain is often the cause of the worst atmospheric attenuation for any frequency regime, the effect of rainfall for V and W band frequencies is especially detrimental. The radius of a rain drop and the wavelengths under consideration are on the same order of magnitude causing severe scattering, in addition to significant liquid water absorption. Also, significant molecular absorption is

incurred in this frequency regime, as several strong molecular absorption lines exist in these bands. To utilize millimeter waves in remote sensing or satellite communication applications efficiently, accurate, long-term attenuation statistics derived using relevant climatology are necessary.

This thesis presents a preliminary investigation into the use of Weather Cubes compiled using the atmospheric characterization package LEEDR for the purpose of acquiring long-term attenuation statistics for satellite communication links. Using input numerical weather prediction (NWP) model data from the National Oceanic and Atmospheric Administration Global Forecast System (GFS), a three-dimensional mesh of physical atmosphere and weather data is created from which radiative transfer parameters can be calculated at each point within the mesh. This allows for the potential inclusion of realistic molecular, aerosol, cloud, and rain effects for a given satellite communication simulation operating at any time and place GFS data is available. The use of LEEDR for radiative transfer calculations makes possible the consideration of systems operating at frequencies in the range 34.9 MHz to 1500 THz (8.6 m to 200 nm wavelength) [4]. Not only does this methodology allow for the potential for communications links to be simulated with environmental conditions it may realistically encounter, but access to daily Numerical Weather Prediction (NWP) data collected over the course of several years also provides a calculated probability of occurrence of a particular weather event. Thus, a satellite communication link can be simulated over an extended period of time to give a better insight on long-term system performance.

1.2 Problem Statement

Propagation loss due to tropospheric effects is a major component of any link budget analysis. The development of future V and W band communication systems requires accurate atmospheric propagation models, which accurately capture lower atmosphere effects, to determine a necessary link margin. With the levels of high attenuation associated

with V and W band attenuation, a reliable atmospheric characterization tool is needed for the testing and evaluation of Propagation Mitigation Techniques (PMT). There is a lack of experimental attenuation measurements at V and W band frequencies, as research into this spectrum for this application has only recently been considered a serious possibility. With the high-cost of experimental campaigns, NWP based models are being considered to supplement the lack of experimental data. While measured data is always needed for validation of a model, a verified and validated NWP based model can be a useful tool for engineers and mission planners.

1.3 Justification

A measurement campaign by Air Force Research Laboratory (AFRL) is focused on measuring attenuation statistics for V and W band frequencies. The campaign consists of three different efforts. The first component consists of radiosounding measurements at AFRL in Rome, NY. These measurements have been published and were available at the time of this research [5] [6]. The second component is a flight test in which a radio beacon transmitting at V and W band will be placed into geo-synchronous orbit. The third test planned will launch a radio transponder that will operate at V and W band. Modeling efforts are needed to support this measurement campaign.

1.4 Approach and Methodology

This research attempts to replicate experimentally measured attenuation data published in [7], with attenuation statistics derived from Weather Cube data at frequencies of 23, 34, 72, and 82 GHz to model the same slant path considered in [7]. Weather Cubes are compiled using a year's worth of NWP data. The total path attenuation is determined for each weather observation event. The total path attenuations from each observation are analyzed statistically to develop a Complementary Cumulative Distribution Function (CCDF) of total path attenuation.

1.5 Assumptions and Scope

This research presents a long-term, NWP based attenuation study considering only four frequencies over a single slant path. In particular, the total attenuation incurred only from aerosol, cloud, molecular, and rain are considered. The scope on this research is restricted by limited availability of measured data and validated models.

1.6 Standards

Accuracy in this research was defined as the error between the measured results derived in [8], and the results derived using the Weather Cube method. The error metric used to evaluate the performance of each trial under consideration is the error figure defined in International Telecommunication Union Radiocommunication Sector (ITU-R) P.311 [9]. This is an accepted standard measure of performance for this type of study [10].

1.7 Research Question

How accurate are 4-D weather cubes at determining long-term attenuation statistics for V and W band frequencies?

1.8 Materials

LEEDR was developed and are maintained by the CDE. Each Weather Cube data set used in this thesis was compiled by researchers at the CDE. The NWP data used to compile the Weather Cubes was taken from NOAA Operational Model Archive and Distribution System (NOMADS). The measurement data used for comparison was provided by AFRL Information Directorate in Rome, NY.

1.9 Other

The sponsor for this research is the AFRL Information Directorate.

II. Background

2.1 Chapter Overview

The development of V and W earth-space links is an active area of research which represents the next evolution in Radio Frequency (RF) system infrastructure. To give context and scope to this research, a brief description of classical link-budget analysis is given. Then a summary of the state-of-the art of V and W satellite communications systems is presented. The formal literature review for this research is divided into three segments. The first segment discusses historical modeling efforts for Extremely High Frequency (EHF). The second summarizes modeling campaigns for V and W band frequencies. The third examines current modeling efforts, with an emphasis on differentiation between various approaches. The chapter concludes with background information on the software used in this research.

2.2 Link-Budget Analysis

The purpose of link-budget analysis is to determine an appropriate operating transmit power P_T level for a given system. The performance of statistical detection and estimation algorithms is a function of the Signal to Noise Ratio (SNR) at the receiver. SNR is defined as the ratio of the power of the transmitted signal P_S to the power of the noise P_N , given by

$$SNR = \frac{P_S}{P_N} \quad (2.1)$$

The total noise power P_N in this work is the contribution of all of the power not originating from the desired source, inclusive of electrical interference, space and atmospheric noise, and other sources. A common system performance metric used in satellite communications is the average probability of bit error or Bit Error Rate (BER), which is defined as the ratio of total number of bits received in error to the total number of bits transmitted. The bit error rate is a function of the SNR at the receiver based on waveform types, encoding

schemes, bandwidth, and other system operating characteristics. The relationship between BER and SNR may be derived theoretically or modeled using a Monte Carlo method. In order for a system to operate at a desired BER, a certain SNR threshold must be achieved. The contributors to the noise power P_N are often random processes not adjustable by the operator. The power at a receiver P_S and a transmitter P_T separated by a distance r are related by the range equation

$$P_S = \frac{P_T G_T G_R \lambda^2}{(4\pi r^2) L_S} \quad (2.2)$$

where λ is the wavelength of the signal, G_T is the gain factor of the transmitting antenna, G_R is the gain factor of the receiver antenna, and L_S is the total path loss [11]. Examining Eq. 2.2 further, the factor of $\frac{\lambda^2}{4\pi r^2}$ accounts for the free space path loss. As this factor is inversely proportional to the square of the carrier frequency, the use of higher frequencies incurs higher free space path loss. The gain-factors of the antennas take into consideration the antenna beam width and directivity. The path loss parameter L_S is the total contribution to all other forms of loss included along the path including atmospheric loss, hardware loss, and other loss factors [11]. The total path loss factor is found as the product of all of the loss constituents. This research is concerned with calculating atmospheric loss L_A , which is a single component of the total path loss L_S in Eq. 2.2. While the other parameters in Eq. 2.2 are considered deterministic, the value used for atmospheric loss is generally derived statistically.

Total atmospheric loss L_A is inclusive of all attenuation incurred on a signal as it propagates from transmitter to receiver. To an earth-space link, the atmosphere is an inhomogeneous propagation medium with composition that varies with altitude. Above 100 km, free-ions and electrons that make up the plasma of the ionosphere can cause significant effects on RF systems. Below an altitude of 100 km, a signal is likely to encounter gaseous water vapor, oxygen and carbon dioxide. Similarly, clouds and rain are most likely found only in the troposphere, at altitudes below 10 km [12]. A profile in this study is a

data point defined for a particular vertical altitude. Profiles of temperature, pressure, and relative humidity vary also in altitude. The atmosphere is considered to be horizontally stratified, as changes in altitude result in large variations of temperature, pressure, and air density while similar changes in horizontal directions (latitude or longitude) often result in negligible differences [13]. Thus atmospheric attenuation calculations can be simplified to only consider functions of one direction [13]. The total atmospheric loss L_A is the summed contribution of total attenuation due to a variety of effects which occur at various altitudes, and are caused by different physical mechanisms. Some of these effects include lower atmospheric effects, such as gaseous, rain, cloud, and aerosol attenuation, tropospheric scintillation, volcanic effects, and upper atmosphere effects such as ionospheric scintillation and Faraday rotation [12]. The methodology developed in this work calculates attenuation from aerosol, cloud, molecular, and rain effects. The statistic commonly used in link budget analysis for lower atmosphere effects is the total attenuation CCDF. Also known as an exceedance curve, a CCDF gives the probability that a given amount of attenuation or loss will be exceeded at any given time. Optimal efficiency and government regulation often requires the minimum acceptable power level to be used, such that a certain performance threshold is met for an acceptable amount of time. To develop an exceedance curve, total path attenuation data must be collected over the course of a time period.

2.3 V and W Band SATCOM

A motivation for using V and W band frequencies in the SATCOM application is the promise of high-bandwidth, yielding a faster data rate. While bandwidth and data-rate are sometimes given the same units (Hz), the two metrics are not equivalent. Bandwidth in (Hz) is a measure of how much frequency content a particular system uses, while data rate is a measure of how much data is passed per second (bits/sec). The definition of bandwidth used in this work is the -3 dB bandwidth, defined as the range in frequencies in which the power of a signal is at least 3dB from the highest power level. In many cases, using

a larger band-width results in a much faster data rate. Alternative ways of increasing data rate include utilizing more advanced communications encoding algorithms, and using more sophisticated software. These methods are often employed in situations in which a user allocated bandwidth is limited, thus the data rate is increased while the bandwidth used remains constant. The use of V and W band frequencies represents a true more bandwidth solution as more spectrum is made available. The large portions of the spectrum allow for very high bandwidth waveforms to be used.

There are no commercial entities currently using V and W band frequencies for uplink or downlink. Various communication structures are being considered for use in V and W band frequencies. A major concern with using these frequencies for satellite communications is the large amount of power that is needed to overcome the extinction due to the troposphere. This will require hardware to operate at an elevated level of efficiency. While the exploration of hardware limitations is not the focus of this research, it is a significant area of concern for designing a future V and W band frequency communications system. Ciancia et.al. states that a communication system operating in the V and W band frequencies will suffer from significant nonlinear distortions and phase noise [3]. To alleviate hardware impairments to a W band communications systems, Sacchi et.al recommends using Pulse Shape Modulation (PSM) using the prolate spheroidal wave function as a waveform [14]. Sanctis et al. also suggests using impulse-radio waveforms for communications systems using V and W band frequencies [15]. Mulinde et.al. recommends overcoming phase noise using single-carrier, constant envelope frequency domain multiple access (SC-CE-FDMA) [16]. SC-CE-FDMA has also been demonstrated to work well in frequency-selective fading channels [16].

With the increase in tropospheric attenuation at higher frequencies, it has become apparent that there is a need for the use of PMT. PMTs include power level, spatial diversity, and adaptive coding. The development of these techniques requires proper

channel characterization. An error model for a quadrature phase shift keyed system is given by Rossi et al. for a satellite communications system utilizing an uplink frequency of 48 GHz, and a downlink frequency of 38 GHz [17]. The error model is based on measurements made during the Alphsat measurement campaign [17]. The Gilbert-Elliott model is intended to support the development of propagation mitigation techniques [17].

2.4 Historical Millimeter Wave Propagation Studies

A seminal report on microwave Earth-Space propagation links was written by Crane and Blood in 1979. This report represents one of the earliest models to use meteorological data, rather than experimental measured data for the prediction of rain attenuation [18]. Addressing effects from molecular, rain, and tropospheric scintillation, the intention of the 1979 report was to address the use of increasingly higher frequencies for earth-space links, which at the time included Ku, K, and Ka band [18]. Using Weather Cubes to derive long-term attenuation statistics, this research intends to provide a methodology to replicate this effort for the V and W band. One of the most significant researchers in the field of millimeter wave propagation was Hans Liebe who developed the Millimeter Wave Propagation Model (MPM). The MPM serves as the basis of many atmospheric line-by-line codes, including the ITU-R recommendation for atmospheric gases (ITU-R P.676) [19].

2.5 Measurement Campaigns in the V and W Band

The measurement of total path attenuation of EHF is an active area of research. Measurement campaigns consist of radiometric studies, and terrestrial and celestial beacon and transponder measurements. A radiometer is a device that measures electromagnetic energy. Radiometric measurements can be post processed to determine attenuation. A beacon measurement consists of determining attenuation by measuring the decrease in power at a receiver from a known transmitter power. A transponder measurement involves the actual transmission of data to determine performance of a particular system. A summary

of millimeter wave propagation studies to-date is given by Murrell et al. [20]. While several preliminary radiometric studies have been published, there is very limited beacon data in the V and W band [20]. The European Space Agency Alphasat satellite transponders have allowed communication experiments at frequencies in the lower portion of the V band (at 47.9 and 48.1 GHz) [17]. There is a significant need for more satellite-based transponder studies. Researchers at the University of New Mexico and the AFRL Space Vehicles Directorate made terrestrial measurements of rain attenuation at V and W band frequencies for a 23 km long slant path, at an elevation angle of 4.16° , using a transmitter and receiver [21]. Measurements of attenuation were made during two, short-term isolated events during a heavy and light rain event at 72 and 84 GHz, and were compared to attenuation data predicted by the Silvia-Mello and ITU-R model for rain attenuation [21]. Another measurement campaign was carried out by the Antennas and Optical Communications Branch of the NASA Glenn Research Center [22]. In this effort, a ground-based radiometer was used to create vertical profiles of temperature and water-vapor up to an altitude of 10 km for an observation period of three months [22]. These vertical profiles were then input to ITU-R recommendations for gaseous and cloud attenuation to solve for total attenuation due to molecular and cloud effects [22]. This method does not allow for the calculation of cloud and rain effects.

Measured attenuation data at frequencies 82, 72, 34, and 23 GHz were derived by researchers from AFRL Information Directorate [8]. An attenuation retrieval algorithm was applied to ground based radiometric measurements over the course of a single year (2011) with a 1 Hz sampling rate [8]. The use of the algorithm allows for the determination of rain attenuation statistics using passive radiometry. The brightness-temperature measurements were made at an elevation angle of 36° from a ground station at Rome, NY [8]. The experimental data collected by Brost et al. is used as comparison data in this research.

2.6 Modeling Campaigns in the V and W band

There are limited modeling capabilities published to support V and W band propagation studies. This is primarily due to the lack of measured data in this frequency regime as many models are developed using measured data. Additionally, empirical or NWP-based modeling techniques require measured data for validation. Atmospheric propagation model types include empirical methods, statistical NWP path attenuation models, and instantaneous NWP path attenuation models [10]. Empirical models are primarily derived from measurements, in which mathematical equations are derived to fit the measured data. Statistical NWP path attenuation models use long-term climatology data collected for exceedance percentage p to calculate attenuation values. Thus, statistical weather data is used to calculate statistical exceedance values. Alternatively, instantaneous NWP path attenuation models directly calculate attenuation from NWP observation data collected over a period of time, which is then used to create an exceedance curve in a method similar to Eq. 3.17.

ITU-R provides recommendations that allow for the calculation of long-term attenuation statistics. An empirical method, ITU-R P. 618 (Propagation data and prediction methods required for the design of earth-space telecommunication systems) is often used in link-budget analysis [23]. Brost and Cook have demonstrated that current empirical methods of calculating the rain attenuation, such as the ITU-R P. 618-10 Model, do not accurately predict rain attenuation in the V and W band [24]. The discrepancies between the empirical models and the available measured data can be partially explained by the fact that the empirical models are derived using lower-frequency data [24]. ITU-R also has published several statistical NWP recommendations for the calculation attenuation from molecular, rain, and cloud effects. These recommendations, along with available climatology published by the ITU-R, are utilized to create comparison data in section 3.6.

The methodology proposed in this thesis is an instantaneous NWP path attenuation model. As a relatively new concept, instantaneous NWP path attenuation models potentially offer desirable advantages over statistical NWP path attenuation models for use in the V and W band. In particular, instantaneous NWP path attenuation models allow for the use of realistically correlated atmospheric and weather data. In statistical NWP path attenuation models, different input climatology exceedance data are collected independently for each attenuation mechanism. As an example, the ITU-R statistical NWP cloud attenuation model (ITU-R P.840) uses the total columnar content of reduced liquid of water vapor for an exceedance percentage data to calculate the attenuation from clouds for a particular exceedance percentage [2]. Simultaneously, an ITU-R statistical NWP path attenuation model for rain determines a specific attenuation from rain that is a function of the rain rate exceeded for a given exceedance probability (ITU-R P.838) to calculate the specific attenuation, and eventually the total path attenuation due to rain [25]. The total columnar content of reduced liquid of water vapor used to calculate attenuation from clouds, and the rain rate used to calculate the attenuation due to rain are then independent of each other, which is not the case in reality [26]. With the significant attenuation incurred from weather effects in the V and W bands, it may be important to preserve the correlation between weather parameters. The calculation of attenuation directly from NWP data allows for this. Additionally, instantaneous NWP-based modeling allows for the consideration of weather diversity along the propagation path.

An instantaneous NWP path attenuation model was developed by researchers from National d'Etudes et de Recherches Aerospatiales. It utilizes GFS data input to Weather Research and Forecasting Model (WRF) to create a four-dimensional data field [27]. The use of the non-hydrostatic WRF allows for a data resolution as low as 20 km at high-computational cost [27]. Using the data field, ITU-R P. 676 is used to calculate molecular specific attenuation from oxygen and water vapor, and ITU-R P.840 is used to calculate

the attenuation from clouds [27]. Specific attenuation from rain is calculated using light scattering theory [27]. Whereas long-term statistics are not provided in [27], a short-term attenuation result is given.

Another instantaneous NWP path attenuation model, Atmospheric Simulator for Propagation Applications (ATM PROP) developed by Lorenzo Luini of Politecnico di Milano, simulates rain and cloud fields using global rainfall and cloud models [10]. ATM PROP creates synthetic rain, cloud, and water vapor fields using data from the European Center for Medium-range Weather Forecast ERA40 database [10]. Rain fields are generated by MultiExcell, Stochastic Model of Clouds, and Stochastic Model of Water Vapor [10]. These synthetic fields of weather data were observed using a weather radar [10]. Whereas a comprehensive verification and validation of ATM PROP has not yet been published, preliminary results are compared with the ITALSAT experiment in [10]. Differences between the instantaneous NWP-based models presented here, and the model presented in this research, will be given in chapter five.

2.7 Weather Cubes and LEEDR

The Weather Cubes used in this research are compiled utilizing LEEDR. A verified and validated atmospheric characterization package and radiative transfer code, LEEDR supports a full spectral range of 34.9 MHz to 1500 THz (8.6 m to 200 nm wavelength) [28]. The development of LEEDR was motivated by the need for highly accurate atmospheric profiles for directed energy weapon simulations. With access to climatology data from the Extreme and Percentile Environmental Reference Tables (ExPERT), LEEDR can create vertical profiles of Weather using relevant climatology [29]. Additionally, LEEDR allows for input atmospheric data from NOMADS, and from several standard reference atmospheres. User-defined weather including different types of rains and clouds can be placed in the atmospheric profile. Weather Cubes extend the functionality of LEEDR to

allow for the consideration of multiple vertical profiles. A description of Weather Cubes is found in literature [4].

III. Methodology

3.1 Chapter Overview

The methodology used to generate long-term statistics from Weather Cubes is given here. To develop this methodology, the calculation of extinction from NWP data is first presented for a single vertical profile. Then the integration of multiple vertical profiles to form a Weather Cube from which total path attenuation calculation is described. An explanation of the ITU-R statistical NWP-based total path attenuation model compared to the Weather Cube derived results is also given. The section concludes with brief description of the error analysis and performance metrics used to compare and contrast different models.

3.2 Attenuation Calculations

The development of total attenuation exceedance curves requires measurements or calculations of total path attenuation over the course of a period of time. In experimental campaigns, signal power received, P , from a beacon transmitting at a known power level P_o is measured. By the Beer-Lambert relationship, the output power P of monochromatic radiation propagating through a medium, with a total extinction coefficient β_e and thickness ΔS is given by

$$P = P_o e^{-\beta_e \Delta Z} \quad [13]. \quad (3.1)$$

Investigating the Beer-Lambert further, the optical depth τ is defined as $\tau = \beta_e \Delta Z$, and the transmittance t is defined as $t = e^{-\tau}$ [13]. To make the connection between attenuation defined in an engineering context and the Beer-Lambert relationship, attenuation is defined as the difference between the incident power of radiation P_o and the output power P

$$A_{dB} = P_{o,dB} - P_{dB}. \quad (3.2)$$

Rearranging Eq. 3.1 yields

$$\frac{P_o}{P} = e^{\beta_e \Delta Z}. \quad (3.3a)$$

Applying the definition of a decibel ($X_{dB} = 10\log_{10}(X)$) to both sides of Eq. 3.3a demonstrates that the left side of Eq. 3.3a becomes the definition of total path attenuation in decibels

$$A_{dB} = 10\log_{10}\left(\frac{P_o}{P}\right) = 10\log_{10}(P_o) - 10\log_{10}(P) = P_{o,dB} - P_{dB}. \quad (3.3b)$$

The right side of equation 3.3a becomes

$$A_{dB} = 10\log_{10}(e^{\beta_e \Delta Z}). \quad (3.3c)$$

To simplify Eq. 3.3c further, the logarithm change of base formula is used. For some ratio X, the change of base formula allows for

$$\ln(X) = \frac{\log_{10}(X)}{\log_{10}(e)}. \quad (3.3d)$$

The change of base formula is substituted in Eq. 3.3c as

$$A_{dB} = 10\log_{10}(e^{\beta_e \Delta Z}) = 10\log_{10}(e)\ln(e^{\beta_e \Delta Z}) = 10\log_{10}(e)\beta_e \Delta Z. \quad (3.3e)$$

The factor $10\log_{10}(e) \approx 4.343$ is known as the attenuation constant. Total path attenuation in decibels is then the product of the attenuation constant and the total optical depth of the system under study which is calculated as

$$A_{dB} = 10\log_{10}(e) * \tau. \quad (3.3f)$$

Thus in experimental campaigns in which the distance ΔZ is known, the extinction coefficient β_e can be calculated. For an experiment measuring total atmospheric attenuation, the extinction coefficient is then constant for the entire earth-space path. As the composition of the atmosphere changes with altitude, the calculated extinction coefficient is generally only representative of total path attenuation. The approach used in this research utilizes the

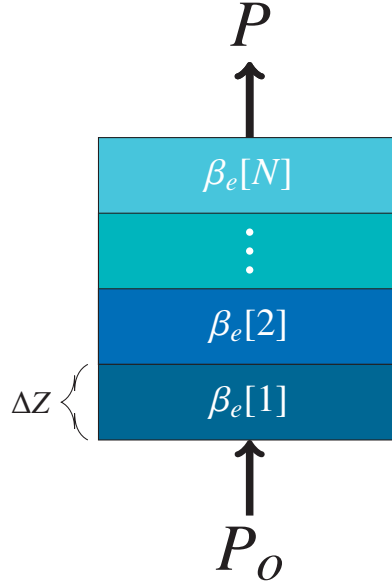


Figure 3.1: Horizontal stratification of the atmosphere. For the purposes of calculating extinction, the atmosphere is divided up into equally spaced layers of vertical width ΔZ .

atmospheric radiative transfer code LEEDR to directly calculate an extinction coefficient inclusive of aerosol, cloud, molecular, and rain effects using first-principle, physical models. Using the horizontal stratification assumption, the atmosphere is divided into N vertical slabs of the same thickness ΔS , in which the composition, temperature, pressure and other physical properties are homogeneous. The spacing of the vertical slabs is based on the resolution of the input profiles used. A graphical representation of this model is given in Fig. 3.1. This allows for a single extinction coefficient to be calculated for a single slab in units of inverse km. The total optical depth for the entire atmosphere is the sum of the optical depth of each slab [13]. For N slabs of equal length, the total optical depth of the atmosphere is given by

$$\tau_{atm} = \sum_{n=1}^N \beta_e[n] \Delta Z. \quad (3.4)$$

The extinction coefficient β_e for each slab is calculated as the sum of extinction due to absorption effects β_a and the total extinction due to scattering effects β_s , given by

$$\beta_e = \beta_a + \beta_s. \quad (3.5)$$

Absorption refers to extinction due to the conversion of signal energy into another form such as heat, and scattering refers to the re-direction of signal energy out of the direction of interest [30]. The total extinction due to absorption β_a is the sum of the extinction due to absorption inclusive of the molecular absorption $\beta_{a,molecular}$, aerosol absorption $\beta_{a,aerosols}$, rain absorption $\beta_{a,rain}$, and cloud absorption $\beta_{a,clouds}$, calculated as

$$\beta_a = \beta_{a,molecular} + \beta_{a,aerosols} + \beta_{a,rain} + \beta_{a,clouds}. \quad (3.6)$$

The total extinction due to scattering β_s is the sum of the extinction due to scattering inclusive of molecular scattering $\beta_{s,molecular}$, aerosol scattering $\beta_{s,aerosols}$, rain scattering $\beta_{s,rain}$, and cloud scattering $\beta_{s,clouds}$, calculated as

$$\beta_s = \beta_{s,molecular} + \beta_{s,aerosols} + \beta_{s,rain} + \beta_{s,clouds}. \quad (3.7)$$

3.2.1 Molecular Absorption.

Molecular absorption is the attenuation due to the conversion of a signal to heat and other chemical energy. The nature of the phenomena is best described using quantum mechanics [13]. The energy of a photon is directly proportional to the frequency f through Planck's constant, given by

$$E = hf. \quad (3.8)$$

A molecular species absorbs photons at specific energies, which translate to specific frequencies according to 3.8. These frequencies are called a variety of names including absorption, spectral, and resonance lines with each line representing a single frequency [13]. Experiments are used to identify and determine the magnitude of spectral lines for various absorption species. The total amount of absorption for a single absorption species

is the summed contribution of each individual spectral line. While absorption lines are defined for single-frequencies, in practice the effect of a single line can cause absorption over a range of frequencies as a result of pressure or Doppler broadening [13]. This effect is captured through the use of line-shapes such as the Gaussian or Lorentzian [13]. Additionally, an absorption continuum is applied to account for differences in between models and measured data [13]. A general equation for total absorption β_{ma} for a given absorption species at given altitude is

$$\beta_{ma} = \rho \sum_{j=1}^J S_j g(f - f_j) + \kappa \quad (3.9)$$

where ρ is the density of the absorption species at a particular layer of the atmosphere, S_j is the strength of the j th spectral line, $g(f - f_j)$ is the line shape, κ is the absorption continuum, and J is the total number of absorption lines under consideration [13]. This methodology is known as line-by-line methodology. As the density of absorption species varies with altitude, Eq.3.9 must be repeated for each altitude in the profile. LEEDR applies a line-by-line method of calculating molecular absorption using spectroscopic parameters from the High-Resolution Transmission Molecular Absorption Database (HITRAN) [31]. Originally created by Air Force Cambridge Research Laboratory, HITRAN is maintained by the Atomic and Molecular Physics Division of the Harvard-Smithsonian Center for Astrophysics [32]. LEEDR considers thirteen different absorption species, which are given in table 3.1 [31].

LEEDR also offers the option of calculating molecular effects using the Correlated-K methodology. A faster calculation alternative to the full line-by-line method, the Correlated-K method averages the contributions of different absorption lines such that the full integration over each line does not have to be considered [13]. Molecular absorption is calculated using a Rayleigh scattering algorithm [31].

Table 3.1: Molecular Absorption Species Used in LEEDR [29]

Absorber	Name	Concentration (Molecule cm ⁻²)
H_2O	Water Vapor	Variable
CO_2	Carbon Dioxide	4.00×10^{-4}
O_3	Tropospheric Ozone	Variable
N_2O	Nitrous Oxide	3.20×10^{-7}
CO	Carbon Monoxide	1.50×10^{-7}
CH_4	Methane	1.794×10^{-6}
O_2	Oxygen	2.09×10^{-1}
NO	Nitrogen Oxide	2.99×10^{-10}
SO_2	Sulphur Dioxide	2.93×10^{-10}
NO_2	Nitrogen Dioxide	2.99×10^{-11}
NH_3	Nitrogen Hydride	5.03×10^{-11}
HNO_3	Nitric Acid	5.30×10^{-11}

3.2.2 Rain and Cloud Absorption and Scattering.

Extinction for rain and clouds is calculated using a Mie scattering algorithm. While a full derivation of the theory of Mie scattering is given in [30], a brief description of the methodology used in LEEDR is given. The implementation of Mie scattering used in LEEDR is the Wiscombe Mie model [33] [31]. Mie Scattering is derived by using a solution to the vector wave equation with spherical polar coordinates for a specific boundary condition [30] [13]. Micro physical properties are assigned to the Mie scattering code based on the rain rate used. The extinction coefficient $\beta_{a,weather}$ is calculated as

$$\beta_{a,weather} = \int_0^\infty n(r)Q_e(r)\pi r^2 dr \quad (3.10)$$

where $n(r)$ is the drop size distribution, r is the radius of a given drop, and $Q_e(r)$ is the extinction efficiency for a single constituent. $Q_e(r)$ is given as

$$Q_e(r) = \frac{2}{r^2} \sum_{n=1}^{\infty} (2n+1)R(a_n + b_n) \quad (3.11)$$

where a_n and b_n are Mie Scattering coefficients [13]. Likewise the extinction due to scattering is calculated by

$$\beta_s = \int_0^{\infty} n(r)Q_s(r)\pi r^2 dr \quad (3.12)$$

where $n(r)$ is the drop size distribution, r is the radius of a given drop, and $Q_s(r)$ is the extinction efficiency for a single constituent. $Q_s(r)$ is given as

$$Q_s(r) = \frac{2}{r^2} \sum_{n=1}^{\infty} (2n+1)R(|a_n|^2 + |b_n|^2) [13]. \quad (3.13)$$

3.2.3 Aerosol Absorption and Scattering .

Aerosols are small particles that are suspended in the atmosphere, such as haze or air pollution. Generally not figured in RF link budget analysis calculations the effects of aerosols could become significant in certain atmospheric conditions for EHF bands. The Wiscombe Mie model is used to calculate aerosol scattering and absorption [31]. Inputs to the model include temperature, relative humidity, radiation frequency, and number density of the aerosol types taken from Global Aerosol Data Set (GADS) [31].

3.3 Calculation of a Slant Path Attenuation

By combining the extinction coefficient from each constituent at each level of the vertical profile using Eq. 3.5, 3.6, and 3.7, a vertical profile of total extinction coefficient is generated. The total path attenuation in decibels, A_{dB} , is calculated as

$$A_{dB} = 10 \log_{10}(e) \sum_{n=1}^N \beta_e[n] \Delta Z \quad (3.14)$$

where N is the total number of points in the profile, $\beta_e[n]$ is the extinction coefficient of the n th slab in units of inverse km, and ΔZ is the vertical thickness of the slab in km. A slant

path is defined as a straight-line path from a platform to target. If a slant path is considered, ΔZ is calculated as,

$$\Delta Z = \frac{L}{N} \sin(\theta) \quad (3.15)$$

The top of the atmosphere in this work is 100 km, as above that altitude the effects calculated using LEEDR are negligible.

3.4 Weather Cubes

A Weather Cube extends the use of a single profile to incorporate weather and atmospheric data for a much larger field of study. A Weather Cube is a data structure that is made up of multiple three-dimensional meshes of data. Each mesh is compiled by the simple concatenation of atmospheric profiles generated using LEEDR for a selected geographic region. An example of a five by five Weather Cube is given in Fig. 3.3, with nomenclature five by five referring to the fact twenty-five total profiles were used in square arrangement of latitude/longitude values. The resulting mesh is a three-dimensional representation of a single type of data, in which each data point is defined at a latitude, longitude, and altitude coordinate.

A description of the Weather Cube data structure is given in Fig. 3.2 for a Weather Cube compiled for a specific time for M latitude and longitude locations, and for vertical profiles calculated for N points. The temperature, relative humidity, pressure, vertical velocity, air density, and relative humidity mesh are created using NWP data from GFS. The C_n^2 mesh is the structure function for atmospheric turbulence calculated using LEEDR's Tatarski Turbulence calculator [31]. The scattering mesh consists of the total extinction from scattering β_s in units of inverse kilometers. Similarly, the absorption mesh consists of the total extinction coefficient from absorption β_a in inverse kilometer. The extinction mesh is simply the sum of the total extinction due to absorption and scattering. The albedo mesh gives the ratio of scattering to absorption at each point. As the calculations of absorption,

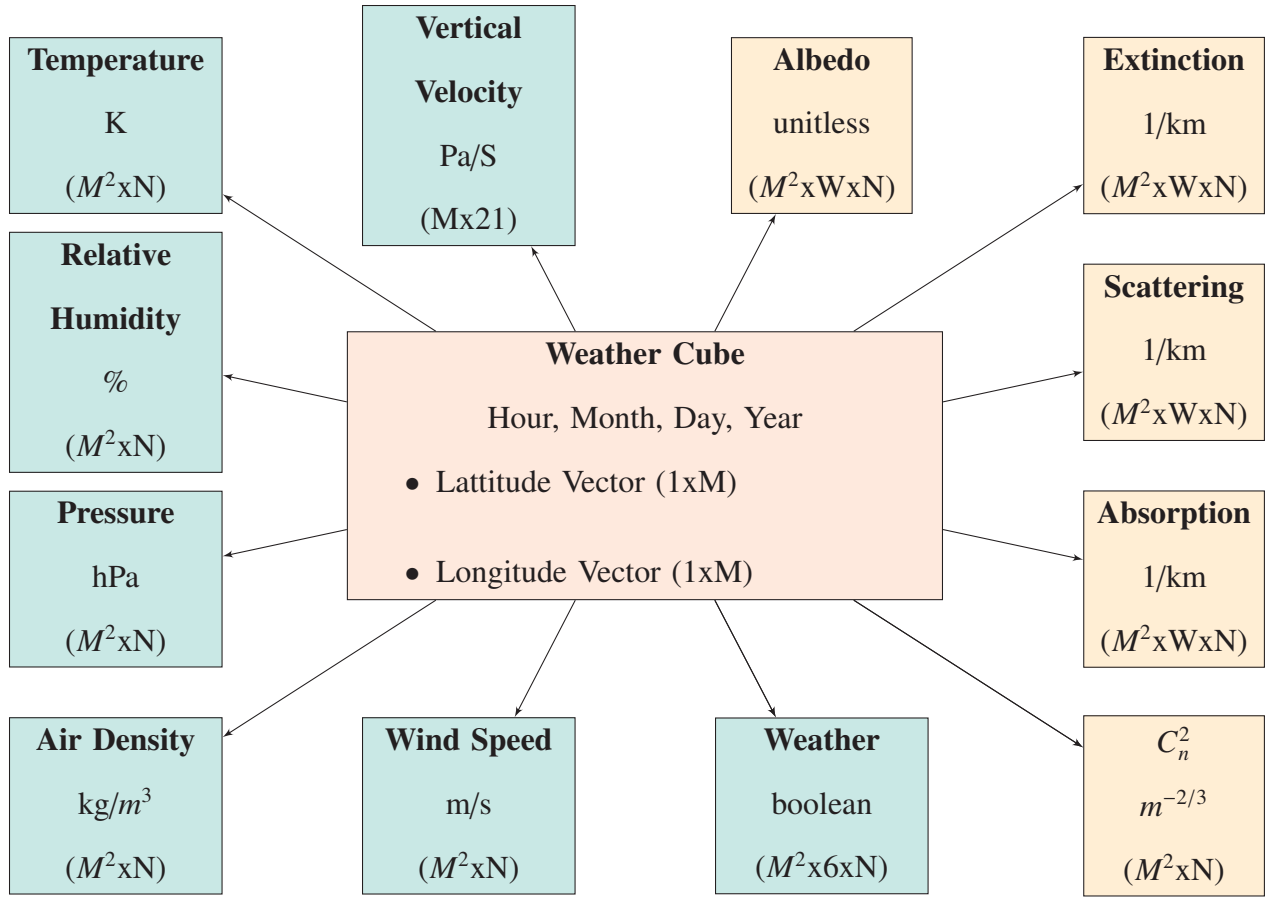


Figure 3.2: Block diagram of a Weather Cube data structure. A single Weather Cube consists of different three dimensional meshes of data, each represented by the boxes in the diagram. The size of each mesh is determined by the number of latitude and longitude points considered M , the number of points in the vertical profile N , and the number of wavelengths (frequencies) considered. Each Weather Cube is defined for a particular date and time.

albedo, total extinction, and scattering are frequency depended, a single mesh is created for each frequency.

GFS data is available at one-half degree latitude by one-half degree longitude for any location on the surface of the earth. GFS data is incorporated into each profile up

to an altitude of 30 km. Above 30 km, atmospheric data is primarily taken from the 1976 Standard U.S. Atmosphere. This is shown in Fig. 3.3, where the green data points indicate portions of each profile in which GFS data is incorporated. GFS is made available four times a day at 0000, 0600, 1200, and 1800 Coordinated Universal Time (UTC) and is available for multiple years.

3.4.1 Physical Size.

The cube size of a Weather Cube is determined by the total number of vertical profiles incorporated. In general, a square number of profiles is used giving rise to the name Weather Cube. Each profile or vertical post extends from the surface to an altitude of 100 km. The physical shape of a Weather Cube is not a perfect cube because of the curvature of the earth. To demonstrate the physical size of a Weather Cube under consideration, a five by five Weather Cube located near Rome, NY is plotted on a north, east, up local level coordinate system in Fig. 3.4. Accounting for the curvature of the Earth, the size of the Weather Cube under consideration is approximately 250 km x 250 km x 100 km. The one-half degree latitude, one-half degree longitude spacing is determined by the NWP data used. With the horizontal stratification of the atmosphere, the limited resolution of data in the north/east plane is generally acceptable.

3.4.2 Weather Placement Algorithm [1].

The GFS data does not provide the necessary details about clouds and rain necessary for the accurate calculation of attenuation. In the absence of meteorological or remote sensing equipment to determine micro-physical properties of clouds and rain, a weather placement algorithm is used. The weather placement algorithm determines at what altitude levels the weather exists and what type of weather exists at each point. Based on the input NWP data, the weather cube algorithm infers that a certain type of reference cloud exists and assigns realistic micro-physical properties. To determine the probable existence of

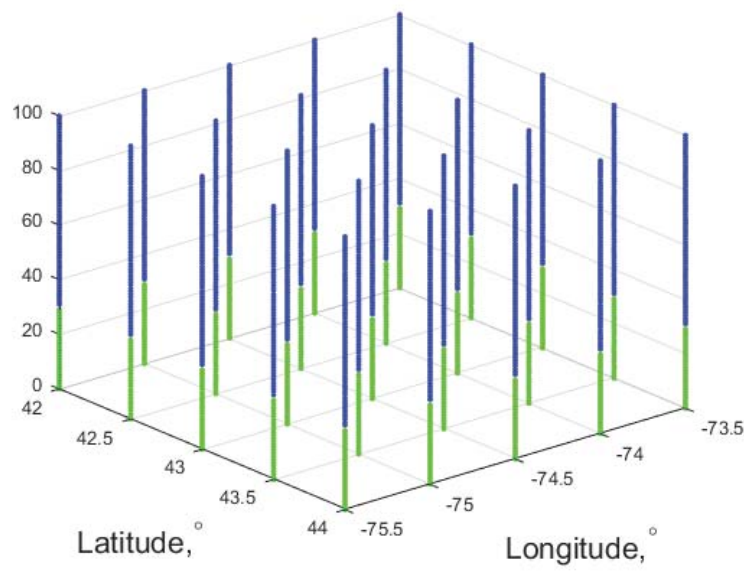


Figure 3.3: An example of a five by five Weather Cube over Rome, NY. Each vertical post or profile extends from the surface to an altitude of 100 km above the surface. The green portion of each vertical post or profile is data taken primarily from GFS data, while the blue portion of each vertical profile is primarily taken from U.S. Standard atmosphere.

clouds at any vertical level as inferred by the GFS model, relative humidity and vertical velocity at each point along the profile are considered. The vertical velocity at each point is the Lagrangian rate of change of pressure. Three different cloud types (fog, stratus, cumulus clouds) can be placed above or below the boundary layer, where the boundary layer is defined as the lowest portion of the troposphere that is in contact with the earth's surface. The thresholds used in the weather placement algorithm are listed in table 3.2 . If the thresholds are met at a particular altitude, then a reference type of cloud is said to exist there.

Rain is placed within the cube if a cloud is determined to exist, and a total precipitation value is reported during the six-hour weather forecast interval. Five different types of rain

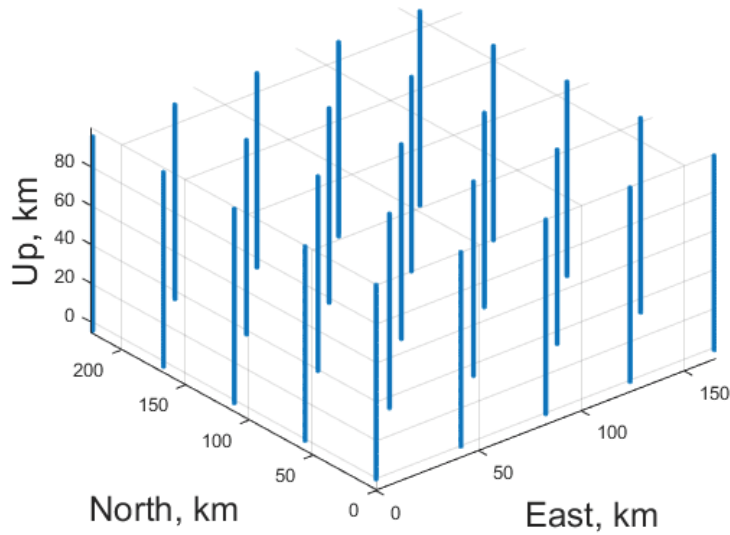


Figure 3.4: The same Weather Cube plotted in Fig. 3.3 is plotted on a north, east, up local level coordinate system, showing the spatial resolution of the data. The location of each vertical profile is determined by the GFS data used to create it. There is approximately 50 km spacing between each profile.

can be placed within the cube including very light rain (2 mm/hr), light rain (5 mm/hr), moderate rain (12.5 mm/hr), heavy rain (25 mm/hr), and extreme rain (75 mm/hr). The total precipitation value reported by the GFS data is divided by six to give a simple average rainfall rate. The intensity of rain placed into the Weather Cube model is determined by the threshold values contained in table 3.3. Rain fields are placed into the vertical profile from the surface up to the half-way point in the clouds. An example of weather fields placed into the Weather Cube is given in Fig. 3.5.

3.4.3 Slant Path Calculations.

The extinction mesh is used to determine the total extinction along the path. An extinction coefficient in units of inverse kilometer is calculated at each data point in the

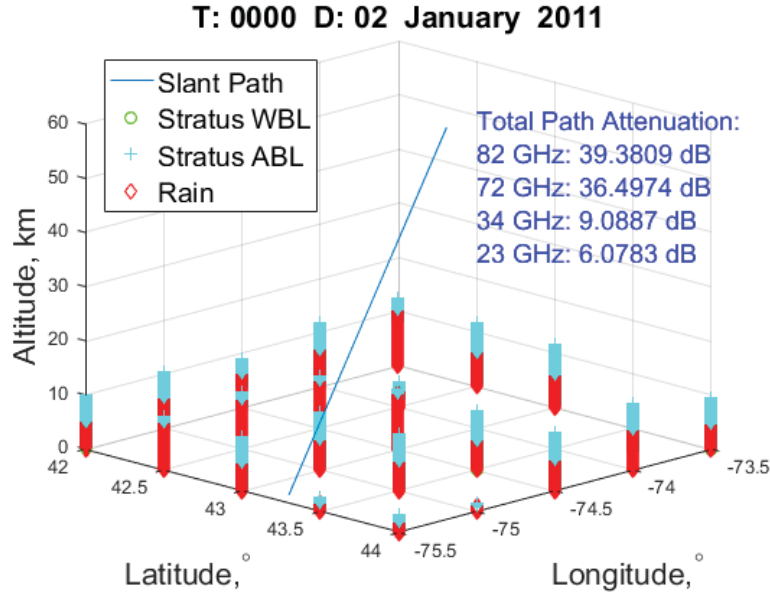


Figure 3.5: An example of weather fields placed inside of a Weather Cube for a single time. Each plotted data point represents a coordinate in which weather (clouds or rain) are placed. The total attenuation values from aerosol, cloud, molecular, and rain effects are given.

mesh. There is a single extinction mesh for each frequency under consideration. A slant path is defined as a straight line path from a platform (transmitter) to target (receiver). The elevation angle is the angle between the slant path and the plane of the surface. The maximum height of each profile in the Weather Cube is 100 km above the surface of the earth, therefore only slant paths up to an altitude of 100 km can be considered. This is acceptable as the effects modeled in the Weather Cubes (aerosols, cloud, molecular, rain) are generally not significant above altitudes of 100 km. In this work, a one-way slant path from a platform located on the surface to a target located at altitude 100 km above the surface is considered. The altitude of each data point in the Weather Cube is given as kilometers directly above the surface.

Table 3.2: Weather Placement Algorithm Thresholds.

Relative Humidity (%)	Vertical Velocity (Pa/s)	Wind Speed (m/s)	Cloud Base (mAGL)	Cloud Type
≥ 100	Upper Limit: 0.00 Lower Limit: -0.12	<2.5	0	Fog
≥ 90	Upper Limit: -0.12 Lower Limit: -5.99	NA	NA	Stratus Within Boundary Layer
≥ 90	Upper Limit: -6.00 Lower Limit: $-\infty$	NA	NA	Cumulus Within Boundary Layer
≥ 70	Upper Limit: -0.12 Lower Limit: -5.99	NA	NA	Stratus Above Boundary Layer
≥ 70	Upper Limit: -6.00 Lower Limit: $-\infty$	NA	NA	Cumulus Above Boundary Layer

When considering a slant path, the curvature of the earth must be taken into effect. The altitude coordinate of each data point in the mesh is given as the altitude directly above the surface. With a curved earth, each point on the surface is at a different altitude relative to every other point on the surface. The Euclidean distance L from a platform located at $(Lat_{plat}, Lon_{plat}, Alt_{plat})$ to a target located at $(Lat_{targ}, Lon_{targ}, Alt_{targ})$, is calculated by converting each coordinate to a Cartesian coordinate system. The slant path is divided into N equally spaced segments of length ΔS according to

$$\Delta S = \frac{L}{N} \quad (3.16a)$$

where N is the resolution of the slant path. The cumulative slant length at the n th point in the slant path is defined as

$$S[n] = \sum_{n=1}^N \Delta S. \quad (3.16b)$$

Table 3.3: Rain Placement Thresholds

GFS Rain Rate (R) (mm/hr)	Weather Cube Rain Rate
$0 < R \leq 3.5$	Very Light Rain ($2mm/hr$)
$3.5 < R \leq 8.75$	Light Rain ($5mm/hr$)
$8.75 < R \leq 18.75$	Moderate Rain ($12.5mm/hr$)
$18.75 < R \leq 50$	Heavy Rain ($25mm/hr$)
$50 < R$	Extreme Rain ($75mm/hr$)

Fig. 3.6 shows the division of a slant path with elevation angle θ into N sections where $S_{alt}[n]$ is the average altitude of the n th slant path segment and

$$\Delta Z = \Delta S * \sin(\theta). \quad (3.16c)$$

Thus the assumption is made that each incremental segment is at a constant altitude which is the simple average altitude of the section. To calculate the average altitude of each section along the slant path, the law of cosines is used. Fig. 3.7 demonstrates the calculation of the elevation along the path where P_{ht} is the height of the platform above the surface of the earth in km, T_{ht} is the height of the target above the surface of the earth in km, and R_E is the radius of the earth (6378.137 km). In the case of earth-space links, the platform height is generally zero as the transmitter is located on the surface. A triangle is formed with vertices at the platform, the target, and the center of the earth as demonstrated in Fig. 3.7.

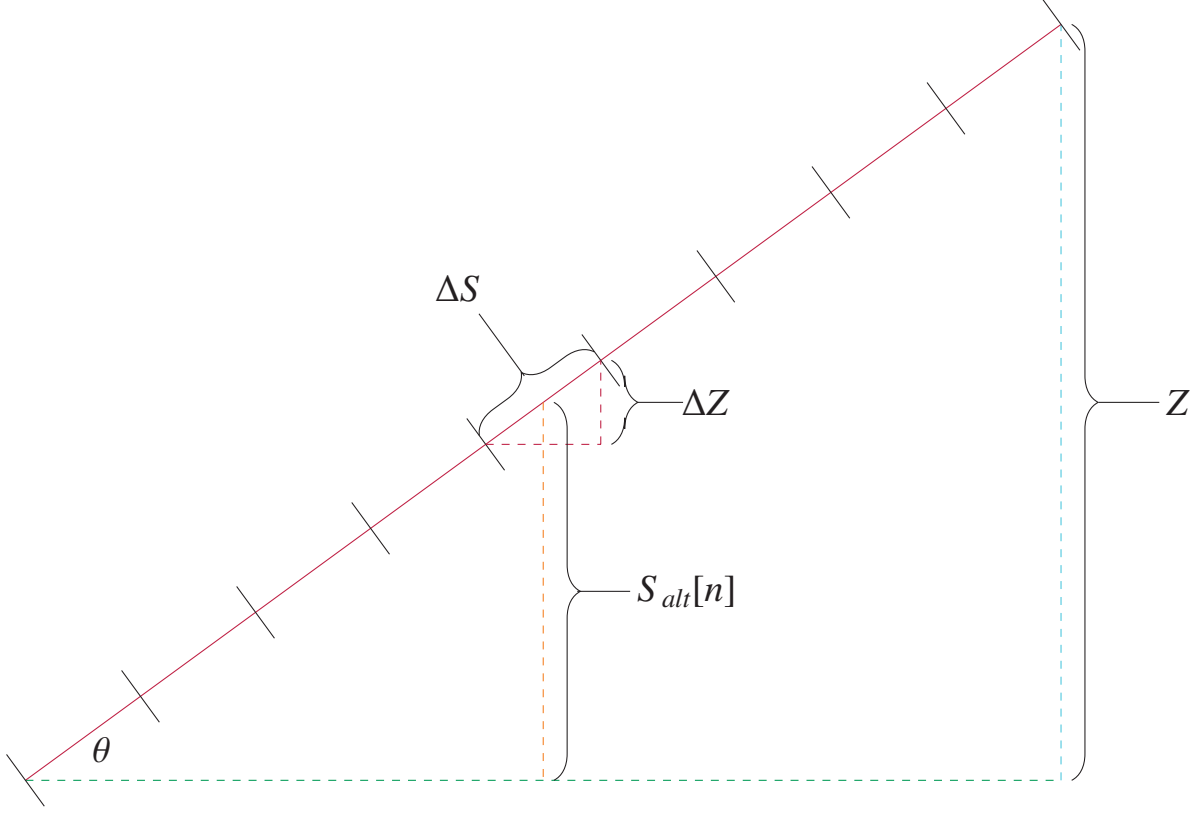


Figure 3.6: Slant path geometry for a straight line path from the surface to an altitude Z at an elevation angle of 36° . The slant path is divided up into N segments of equal length ΔS . The altitude of n th segment $S_{alt}[n]$ is the average altitude of the segment.

The length of two sides of the triangle are given by

$$P_{ht+R} = P_{ht} + R_E \quad (3.16d)$$

and

$$T_{ht+R} = T_{ht} + R_E. \quad (3.16e)$$

The parameter $\cos(\phi)$ is calculated as

$$\cos(\phi) = \frac{T_{ht+R}^2 + L^2 - P_{ht+R}^2}{2T_{ht+R}L} \quad (3.16f)$$

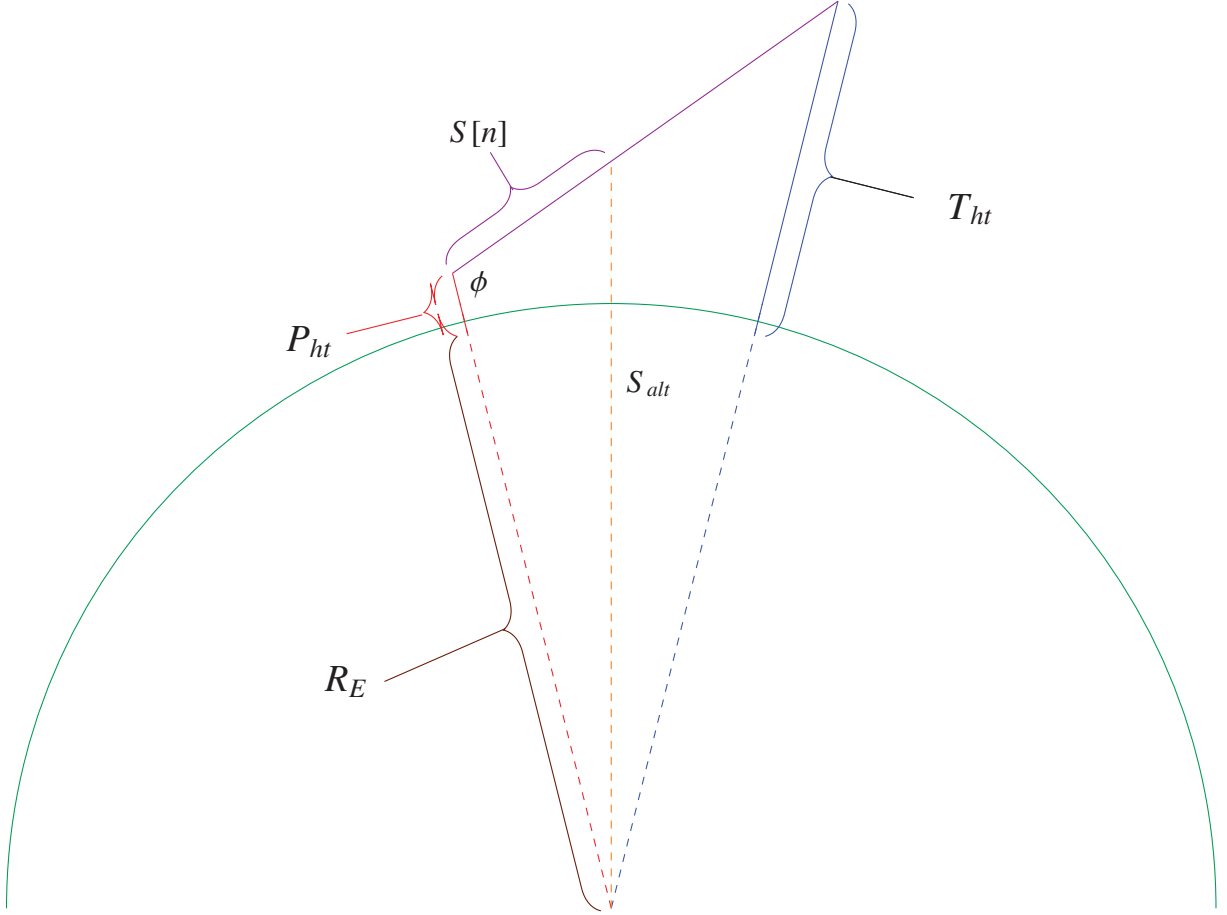


Figure 3.7: Calculation of altitude at each point along the slant path between a platform with altitude P_{ht} and a target at altitude T_{ht}

The distance from the center of the earth to the position of the nth point in the slant path is calculated as

$$A_{S+R}(n) = \sqrt{P_{ht+R}^2 + S[n]^2 - 2S[n]P_{ht+R}\cos(\phi)} \quad (3.16g)$$

where $S[n]$ is defined in Eq. 3.16b. To get altitude above the surface, the radius of the Earth is subtracted out in

$$A_S = A_{S+R} - R_E. \quad (3.16h)$$

The altitude of each incremental length is the average altitude for each segment along the slant path calculated as

$$S_{alt}[n] = \frac{S[n] + S[n+1]}{2}, \text{ for } n = 1, 2 \dots N-1. \quad (3.16i)$$

$S_{alt}[n]$ is the altitude of the n th segment. The slant path then is defined as the set of N total coordinates $(S_{lat}[n], S_{lon}[n], S_{alt}[n])$, where $S_{lat}[n]$ and $S_{lon}[n]$ are the latitude and longitude coordinates of the midpoint of the n th slant path section. A three-dimensional, linear interpolation of the three-dimensional extinction mesh is used to determine an extinction coefficient $\beta_e[n]$ for each coordinate in the slant path. Any portion of the slant path which lies outside of the geographic boundary of the Weather Cube is assigned an extinction coefficient of zero. Any slant path, regardless of elevation angle or whether it passes through a given profile, can be considered with this methodology.

3.5 Long-Term Statistics

Each Weather Cube is compiled for a single date and time according the availability of the NWP data. With the GFS data used in this study, it is possible to create an array of Weather Cubes by collecting Weather Cubes compiled over the course of desired period of time. With the GFS data used in this study, individual Weather Cubes can be compiled four times a day (at 0000, 0600, 1200, and 1800 UTC) for any day in which GFS data is available. To develop long-term attenuation statistics for a given slant path, the total attenuation for the path is simply calculated for each Weather Cube in the array. The incorporation of NWP over a wide range of dates allows for the calculation of attenuation values necessary for the calculation of total path attenuation probability of exceedance curves. To calculate the exceedance curve from the Weather Cube attenuation, a combinatoric method under a uniform probability distribution assumption is used in,

$$EX(m) = \frac{\# \text{ of } (A > (A(m)))}{M}, \text{ for } m = 1, 2, 3 \dots M \quad (3.17)$$

where $EX(m)$ is the exceedance probability of the attenuation value calculated from the m th Weather Cube, $A(m)$ is the total path attenuation calculated for the m th Weather Cube, and M is the total number of Weather Cubes in the array.

3.6 International Telecommunication Union Recommendations

The ITU-R publishes several recommendations for the planning of earth-space links. To provide another comparison in addition to the measured data, several ITU-R recommendations are combined. The recommendations used in this comparison are given in table 3.4. Whereas the ITU-R recommendations are updated periodically, the recommendations used in this work were the most up-to-date at the time of this analysis. The ITU-R does not provide a recommendation for aerosol attenuation, as the effects of aerosols are not generally factored into link-budget calculations. The total path attenuation is found by combining the recommendations for molecular (gaseous), cloud, and rain effects. Full descriptions of the calculations used in each ITU-R recommendation are published, therefore these descriptions will not be repeated here. Instead, the integration of the different recommendations used to derive the data is presented .

Table 3.4: ITU-R Recommendations Used in this Work

Recommendation	Name	Last Update
ITU-R P.676-11	Attenuation by Atmospheric Gases	9/16
ITU-R P.835-5	Reference Standard Atmospheres	2/12
ITU-R P.837-7	Characteristics of Precipitation for Propagation Modelling	6/17
ITU-R P.838-3	Specific Attenuation Model for Rain for Use in Prediction Methods	3/15
ITU-R P.839-4	Rain Height Model for Prediction Methods	9/13
ITU-R P.840-6	Attenuation Due to Clouds and Fog	9/13
ITU-R P.1511-1	Topography for Earth-to-Space Propagation Modelling	8/15

3.6.1 ITU-R Molecular Absorption .

ITU-R P.676-11 is implemented to calculate molecular effects [34]. The full, line-by-line summation is used. As compared to Weather Cube methodology, ITU-R P.676-11 considers only resonance lines from oxygen and water vapor with a dry and wet continuum [34]. Inputs to ITU-R P.676-11 include the temperature profile in K, atmospheric pressure profile in hPa, and the water vapor partial pressure profile. Each of these profiles is taken from the U.S. Standard Atmosphere from ITU-R P.835-5 [35]. Each profile includes data from the surface to an altitude of 85 km above the surface, with a resolution of 85 m. For each datapoint in the vertical profile, a specific attenuation value is calculated with units (dB/km). The total gaseous attenuation for a slant path in decibels is calculated by

$$A_{gas} = \sum_{n=1}^N \gamma_m[n] \Delta Z \quad (3.18)$$

where $\gamma_m[n]$ is the specific attenuation due to gaseous absorption of the n th point in a profile, N is the total number of vertical points in the profile, and ΔZ is defined in Eq.3.15.

3.6.2 ITU-R Cloud Absorption [2].

ITU-R P.840-6 is implemented to calculate the exceedance curve for cloud effects. ITU-R P.840-6 directly calculates the total attenuation due to cloud effects for a given exceedance probability by

$$A_{Cloud}(p) = \frac{L_{red}(p)K_l}{\sin(\theta)} \quad (3.19)$$

where L_{red} is annual the total columnar content of reduced liquid of water vapor for an exceedance percentage p , K_l is a frequency dependent term, and θ is an elevation angle. Climatology values for L_{red} for a specified latitude and longitude coordinate are provided through a digital map for exceedance probabilities 0.1, 0.2, 0.3, 0.5, 1, 2, 3, 5, 10, 20, 30, 50, 60, 70, 80, 90, 95, and 99 %.

3.6.3 ITU-R Rain Effects.

To calculate the exceedance curve for rain, data from several ITU-R recommendations are combined. The total rain attenuation exceedance curve for a given probability p is given

by

$$A_{rain}(p) = \gamma_{rain}(p) \frac{(h_r - h_s)}{\sin(\theta)} \quad (3.20)$$

where h_r is the mean annual rain height above mean sea level in km, h_s is topographical height, θ is the elevation angle, and $\gamma_{rain}(p)$ is the specific attenuation due to rain for an exceedance percentage p . Values for h_r and h_s for a particular latitude and longitude coordinate are taken from digital maps in recommendation ITU-R P. 839-4 and ITU-R P. 1511-1 respectively [36] [37]. To calculate $\gamma_{rain}(p)$ ITU-R P.838-8 is used. Inputs to ITU-R P.838-8 include rain rate exceeded for a given probability p , frequency, elevation angle, and polarization angle [25]. A polarization angle of 45° is assumed. The rain rate exceeded for a given probability p for a given latitude and longitude coordinate is taken from ITU-R P.837-7 [38].

3.6.4 Total ITU-R Attenuation .

The exceedance curve for the total path attenuation due to the effects of cloud, rain, and molecular attenuation $A_{total}(p)$ is calculated as

$$A_{total}(p) = A_{gas} + A_{cloud}(p) + A_{rain}(p) \quad (3.21)$$

where A_{gas} , A_{cloud} , and A_{rain} are all described previously. A constant molecular attenuation value, A_{gas} , is assumed since the 1976 U.S. standard atmosphere is used rather than a series of NWP data. To generate the exceedance curve, Eq: 3.21 is applied to 500 equally spaced exceedance probability values from 0.01 % to 99 %. To demonstrate this methodology, the ITU-R method is used to create an exceedance curve for Rome, NY. The ITU-R derived exceedance curve is plotted in 3.8 against the exceedance curves generated using radio-sound data in [8].

3.7 Model Error Figure

The metric used to determine how well the Weather Cube method calculates total path attenuation as compared to other methodologies is the error figure given in ITU-R P.311.

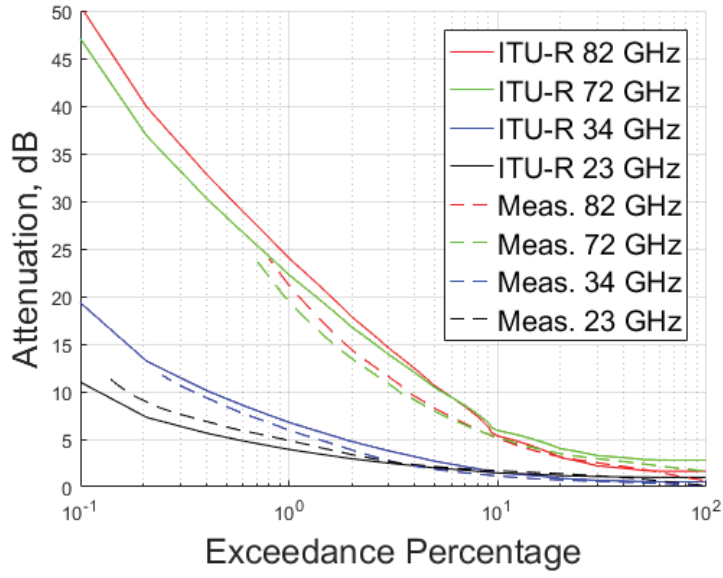


Figure 3.8: Comparison of extinction curves derived using the ITU-R methods plotted with experimental data collected in [8].

The error figure for a given exceedance percentage p , $\psi(p)$ is calculated as

$$\psi(p) = \begin{cases} \left(\frac{A_{ref}(p)}{10} \right)^{0.2} \ln \left(\frac{A_{exp}(p)}{A_{ref}(p)} \right) & \text{if } A_{ref}(p) < 10 \text{ dB;} \\ \ln \left(\frac{A_{exp}(p)}{A_{ref}(p)} \right) & \text{if } A_{ref}(p) \geq 10 \text{ dB.} \end{cases} \quad (3.22)$$

where $A_{ref}(p)$ is the reference, and A_{exp} is the experimental attenuation value at percentage p [9]. The average error figure in the this research is defined as the simple arithmetic average across $\psi(p)$, and the root mean square error is defined similarly.

IV. Results Analysis

4.1 Introduction

To evaluate the use of Weather Cubes to determine long term statistics, exceedance curves are generated using the methodology developed in section 3.5 for a 36° slant path in Rome, NY. All results are derived for a one-way path from the ground to a point 100 km above the surface of the earth. The decision to model a slant path from Rome, NY is motivated by the availability of ground based radiometric measurements of slant path attenuation data in the V and W band to compare against [8]. The four frequencies considered in each trial are 82, 72, 34, and 23 GHz.

Results are reported as four different trials which use different combinations of Weather Cube size and number of years of NWP data. The research efforts are described in table 4.1. As this research represents a first attempt to develop long-term statistics using Weather Cubes, a significant amount of this effort was invested into troubleshooting. Total path attenuation probability of exceedance curves are generated for each frequency in each trial. The performance of each trial is quantified through the ITU-R error figure, the calculation of which is described in section 3.7. Additionally, the average and the root-mean-square value of the error figure for each frequency is given for each trial. The attenuation due to aerosols was found to be negligible at these wavelengths, therefore those results will not be presented here.

4.2 Trial One

For an initial trial, a three by three Weather Cube was implemented. GFS profiles in a mesh of 42° to 44° latitude, and -75.5° to -73.5° longitude with a one-half degree resolution were used. The latitude and longitude coordinates were chosen such that the center of the Weather Cube was located near Rome, NY. The GFS data used was collected four times

Table 4.1: Overview of Configurations Considered in this Research

Experiment #	Size of Weather Cube	Years of GFS Data Used
1	3x3	2: (2015,2016)
2	1x1	2: (2015,2016)
3	1x1	1 (2011)
4	5x5	1 (2011)

a day (0000, 0600, 1200, 1800 UTC) for each day for the years 2015 and 2016. Omitting erroneous NWP reports, a total of 1,395 observations were used. Erroneous reports are weather observation events in which no data is available from GFS. The exceedance curves derived using the full weather cube compared with the exceedance curves measured in [8] are given in Fig. 4.1.

4.2.1 Trial One Results .

The resulting attenuation curve calculated in trial one was an order of magnitude different than the results derived experimentally in [8]. The behavior of the 82 GHz and the 72 GHz exceedance curve was also very different relative to each other, as compared to the measured data. As the results derived in trial one are clearly erroneous, no error analysis will be considered. The cause of the significant error between the two models is the use of the correlated-k methodology to calculate molecular effects. A plot of the total molecular attenuation calculated by the line-by-line molecular absorption, as compared to that calculated by the correlated-k method across a frequency sweep of the V and W band is given in Fig. 4.2. As is demonstrated in Fig.4.2, the band-averaging correlated-k method does not adequately capture the effects of the many resonance lines around 60 GHz, resulting in the large difference between the methodologies. It is recommended that

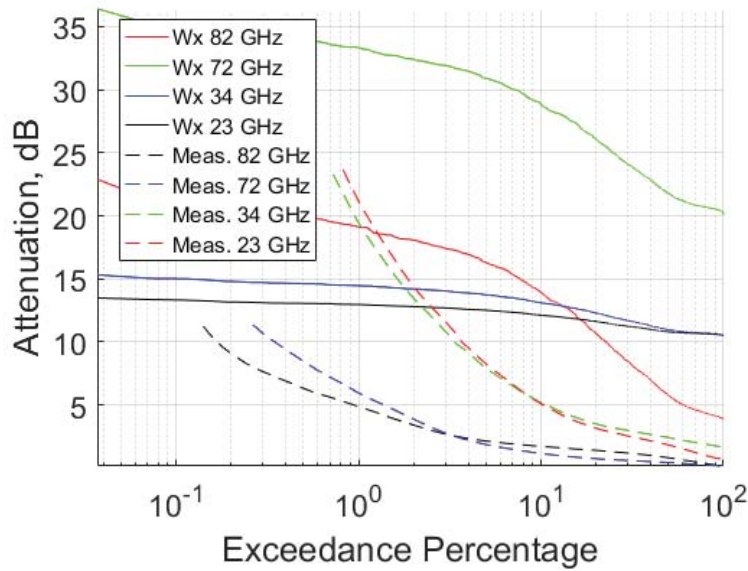


Figure 4.1: Trial One: Exceedance curves derived using a three by three Weather Cube using two years of NWP data as compared to the experimental results derived in [8]. The results are plotted on a logarithmic scale on the independent axis to emphasize the difference in the highest attenuation values occurring at the lowest exceedance percentages. The results derived using the Weather Cube data do not show agreement with the measured data.

full line-by-line molecular absorption methods should be implemented in the V and W band.

4.3 Trial Two

A single GFS profile located at 43.0° latitude and -75.5° longitude was considered for two years of data. The latitude and longitude coordinate used is located near Rome, NY. The GFS data used was collected four times a day (0000, 0600, 1200, 1800 UTC) for each day in the year 2015 and 2016. Omitting erroneous NWP reports, a total of 2696 observations were used. The exceedance curves derived using the single-profile for two years with the

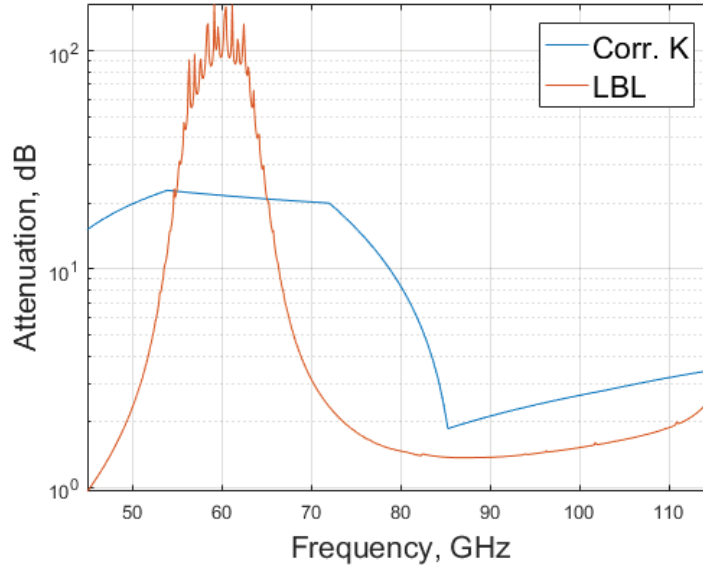


Figure 4.2: Total path attenuation from molecular effects calculated using a line-by-line (LBL) and Correlated-K at (Corr.K) at cm^{-1} resolution for a frequency sweep of the V and W band.

exceedance curves measured in [8] is given in Fig. 4.8. For the second trial, LEEDR output profiles of molecular, rain, cloud, and aerosol extinction were generated allowing for comparisons to corresponding ITU-R methods described in section 3.6. The use of LEEDR output profiles allows for each constituent effect to be considered individually. The Weather Cube data structure does not include separate extinction profiles for each constituent effect, as the extinction data included in the Weather Cube data structure is the total combined path extinction.

4.3.1 Trial Two Results.

The use of the line-by-line method to calculate molecular absorption gives much more accurate results, as compared to the results obtained in trial one. The exceedance curve generated in trial two is given in Fig. 4.3. The error figure curve given in Fig. 4.4 plots the error figure $\psi(p)$ for each exceedance probability p . Fig. 4.4 shows that the maximum error

occurs at approximately $p = 10\%$ with the relatively low error occurring at the highest exceedance percentages. The comparison between the ITU-R model for molecular effects (ITU-R P.676) and the molecular effects derived from the Weather Cube model is given in Fig. 4.5. As the molecular effects in the ITU-R are calculated using standard atmospheres, the total attenuation values are constant for each exceedance percentage. The comparison between the ITU-R cloud model derived probability of exceedance and the Weather Cube model given in Fig. 4.6 shows good agreement at low exceedance percentages with more variation at higher exceedance percentages. The comparison between the total rain attenuation exceedance curves calculated by the Weather Cube methodology given in Fig. and the ITU-R model show the greatest discrepancy. The largest attenuation values of any effect are the result of rain. When only a single profile of NWP data is used, there is only one type of weather incorporated into the entire slant path for each weather observation event. This is likely the cause of the stair-case like shape of Fig. 4.3, as there is no weather diversity in the path.

Table 4.2: Trial Two: Error Figure Statistics

Frequency	MEAN	RMS
GHz	ψ	ψ
82	0.4991	0.6811
72	0.4686	0.6317
34	0.3837	0.5151
23	0.1175	0.2072

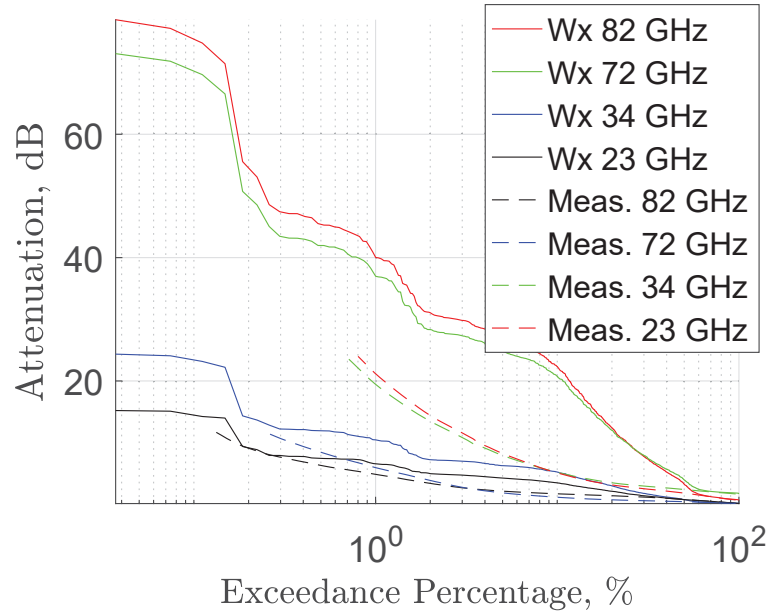


Figure 4.3: Trial Two: Exceedance curves derived using a single profile with two years of NWP data as compared to the experimental results derived in [8]. The results are plotted on a logarithmic scale on the independent axis to emphasize the difference in the highest attenuation values occurring at the lowest exceedance percentages.

4.4 Trial Three

A single GFS profile located at 43.0° latitude and -74.5° longitude was considered for a single year of data. The latitude and longitude coordinate used are approximately at the midpoint of the slant path modeled in [8]. The GFS data used was collected four times a day (0000, 0600, 1200, 1800 UTC) for each day in the year 2011. Omitting erroneous NWP reports, a total of 1,395 observations were used. The purpose of considering a single slant path for a single year is to provide comparison data for both a single-profile trial described in section 4.3, and the full five-by-five cube considered in section 4.4.1. The exceedance curves derived using the single-profile for a single year with the exceedance curves measured in [8] is given in Fig. 4.8.

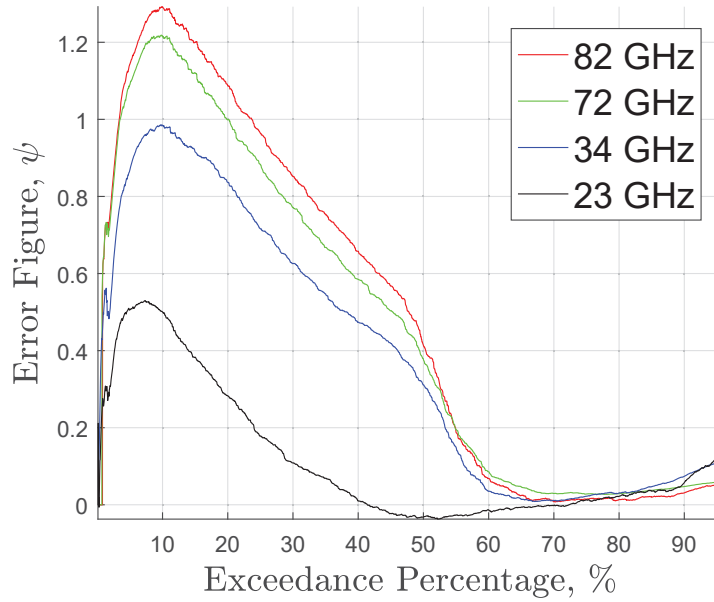


Figure 4.4: Trial Two: Error figure between the exceedance curves calculated using Weather Cubes and those observed experimentally in [8]. The error figure is defined in section 3.7. The maximum error occurs between five and fifteen percent.

4.4.1 Trial Three Results .

The error figure generated for trial three is given in Fig. 4.9, and the table containing the average and RMS values for the error figure of each frequency is given in table 4.3. As compared to the results derived in trial two (single profile, two years of NWP data), there is an increase in the average error figure across all results. The GFS data used to create each Weather Data is available for only four times a day, giving a six hour temporal spacing of the calculated attenuation data. The measured attenuation data was derived from a radio sound technique, which made measurements at a sampling frequency of 1 Hz [8]. The Weather Cube data is sparsely sampled as compared to the measured data. Using more years of NWP data, and thus more Weather Cubes, should allow for a greater variety of weather observations to be incorporated into the total attenuation statistics. Including more

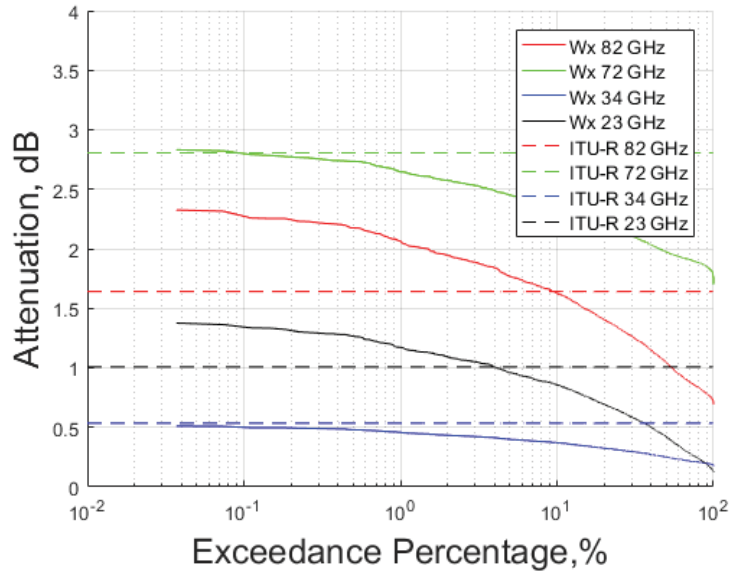


Figure 4.5: Comparison of ITU-R and Weather Cube molecular attenuation models for the calculation of attenuation extinction curves from molecular absorption and scattering.

weather observations increases the chance of capturing significant rain and cloud events, which will likely result in a more realistic exceedance curve. Whereas there is a limit on how accurate the Weather Cube method can be based on the use of six hour GFS data, the additional high-attenuation events observed should produce a more accurate distribution of attenuation data from which to calculate the total exceedance.

4.5 Trial Four

A full five by five Weather Cube was implemented. GFS profiles in a mesh of 42° to 44° latitude and -75.5° to -73.5° longitude with a one-half degree resolution were used. The latitude and longitude coordinates were chosen such that the a full slant path pointing directly east originating from the surface at Rome, NY to an altitude of 100 km above the

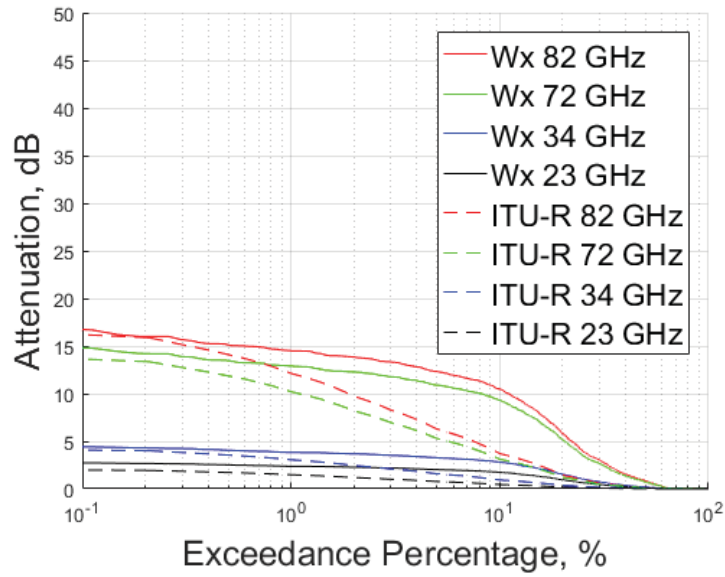


Figure 4.6: Comparison of ITU-R and Weather Cube cloud attenuation models for the calculation of attenuation extinction curves from cloud absorption and scattering.

Table 4.3: Trial Three: Error Figure Statistics

Frequency GHz	MEAN ψ	RMS ψ
82	0.5204	0.7289
72	0.4941	0.6770
34	0.4064	0.5569
23	0.1414	0.2373

surface. This geometry was chosen to attempt to replicate the propagation path used in [8]. The GFS data used was collected four times a day (0000, 0600, 1200, 1800 UTC) for each day in the year 2011. Omitting erroneous NWP reports, a total of 1395 observations

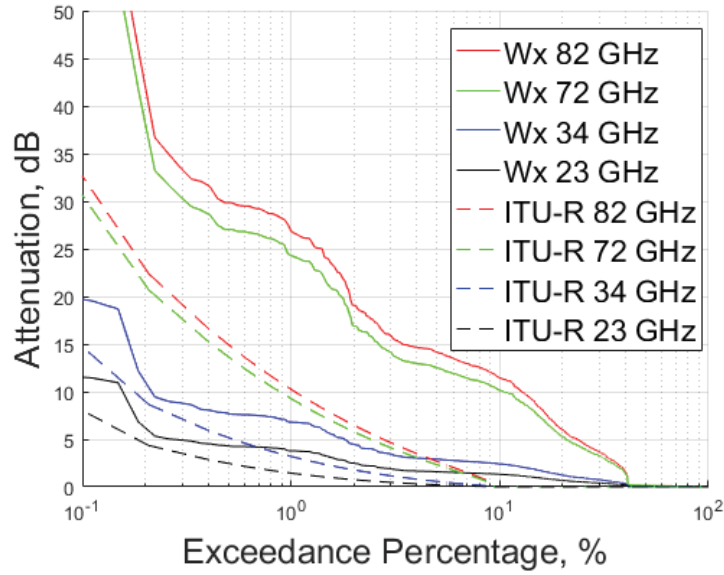


Figure 4.7: Comparison of ITU-R and Weather Cube rain attenuation models for the calculation of attenuation extinction curves from cloud absorption and scattering.

were used. The exceedance curves derived using the full Weather Cube compared with the exceedance curves measured in [8] is given in Fig. 4.10.

4.5.1 Trial Four Results.

The error figure generated for trial four is given in Fig. 4.11, and the table containing the average and RMS values for the error figure of each frequency is given in table 4.4. Across all results, the average and RMS of the error figure are larger then in the both single profile, single year case (trial three), and the single profile double year case (trial four).

4.6 Best and Worst Case Analysis

For further analysis an examination of individual observations is given. In particular, the worst case scenario and best case scenario attenuation events are considered. The worst case scenario in this study is the observation in which the highest total path attenuation

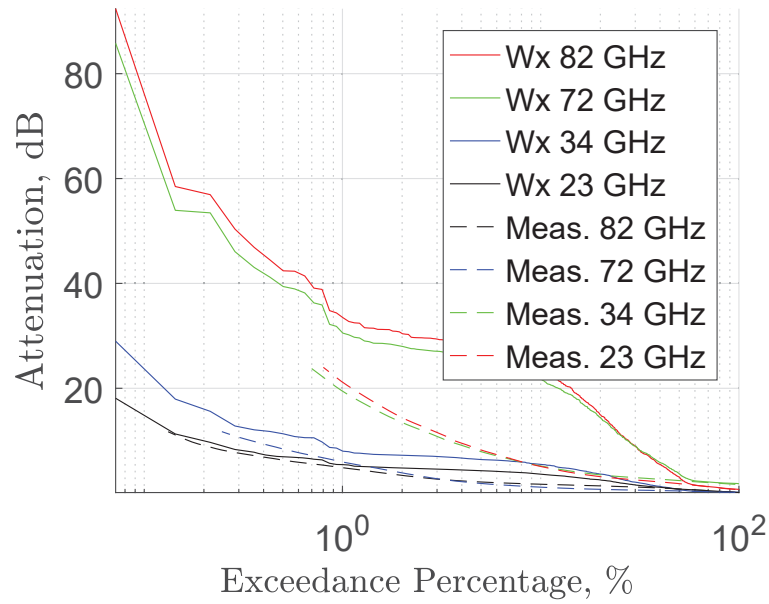


Figure 4.8: Trial Three: Exceedance curves derived using a single profile with a single year of NWP data as compared to the experimental results derived in [8].

Table 4.4: Trial Four: Error Figure Statistics

Frequency GHz	MEAN ψ	RMS ψ
82	0.5766	0.7811
72	0.5365	0.7237
34	0.4552	0.5984
23	0.1688	0.2718

values is observed. With the effects considered in this research, the worst case scenario is the day in which the most extreme rain event is observed. The worst case scenario captured in 2011 by a Weather Cube for Rome, NY occurred on August 28th, 2011. A depiction

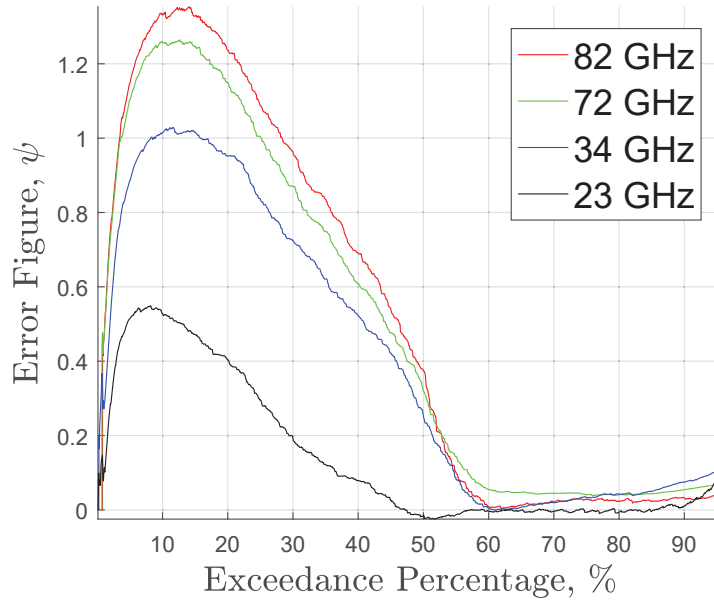


Figure 4.9: Trial Three: Error figure between the exceedance curves calculated using Weather Cubes and those observed experimentally in [8]. The error figure is defined in section 3.7. The maximum error occurs between five and fifteen percent.

of the rain fields placed in the cube is given in Fig. 4.12. The total attenuation values for the worst case are 82 GHz and 72 GHz are given as 88.4 dB and 82.1 dB respectively. A plot of the extinction coefficient along the slant path is given in Fig. 4.13. After a distance of approximately 25.5 km along the slant path (a distance of approximately 21 km across the surface), the extinction coefficient drops to zero. The best case attenuation event is the observation in which the least attenuation is observed. The least attenuation is observed under clear sky conditions. The least attenuation observed captured in 2011 by a Weather Cube for Rome, NY occurred on February 15th, 2011, and is depicted in Fig. 4.14. A plot of the extinction curve along the slant path is given in Fig. 4.15. The total attenuation values for the best case are 82 GHz and 72 GHz are given as 1.2 dB and 3.2 dB respectively. The dynamic range, defined as the difference between the largest attenuation and the least

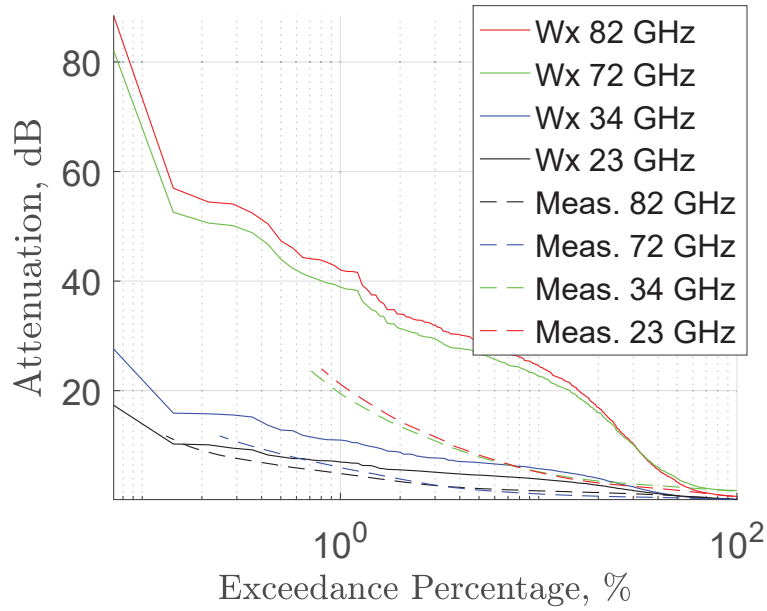


Figure 4.10: Trial Three: Exceedance curves derived using a full five by five Weather Cube compared to the experimental results derived in [8].

attenuation calculated by the Weather Cubes, is 84.4, 87.2, 21.5, and 78.9 dB respectively

4.7 Full Results Analysis

The total error results as compared to measured results are given in table 4.5. To show the distribution of attenuation values calculated using the Weather Cubes, Fig. 4.17 gives a histogram of total path attenuation data for the 82 GHz frequency in the Weather Cube. The use of a full five by five weather cube incurs slightly more error than a single weather profile for the same year. This conclusion is counter-intuitive, as one might expect the use of the full five by five Weather Cube should allow for a diversity of weather along the slant path. The cause of this discrepancy might be best explained by examining each constituent effect

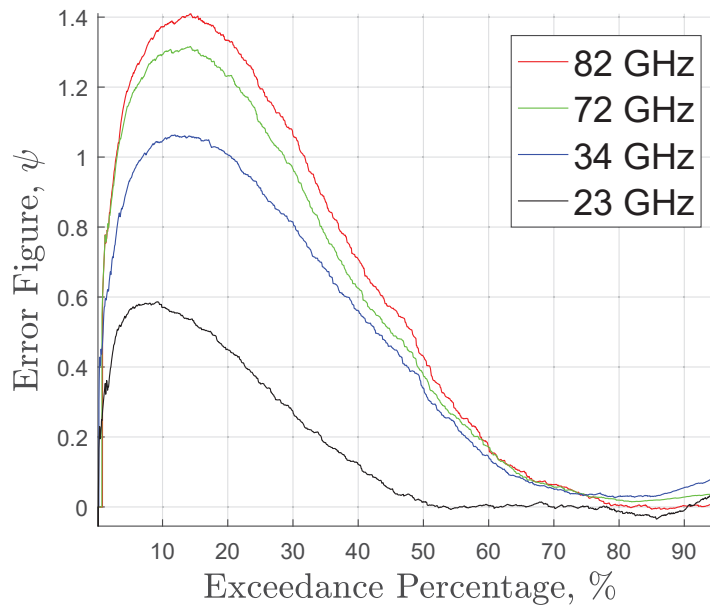


Figure 4.11: Trial Four: Error figure between the exceedance curves calculated using Weather Cubes and those observed experimentally in [8]. The error figure is defined in section 3.7. The maximum error occurs between five and fifteen percent.

Table 4.5: Summary of Error Results from Each Trial

Frequency	Trial 2	Trial 3	Trial 4
GHz	MEAN ψ	MEAN ψ	MEAN ψ
82	0.4991	0.5204	0.5766
72	0.4686	0.4941	0.5365
34	0.3837	0.4064	0.4552
23	0.1175	0.1414	0.1688

separately. As demonstrated in trial two, the total attenuation calculated by rain showed the greatest difference between the Weather Cube derived results and the results suggested

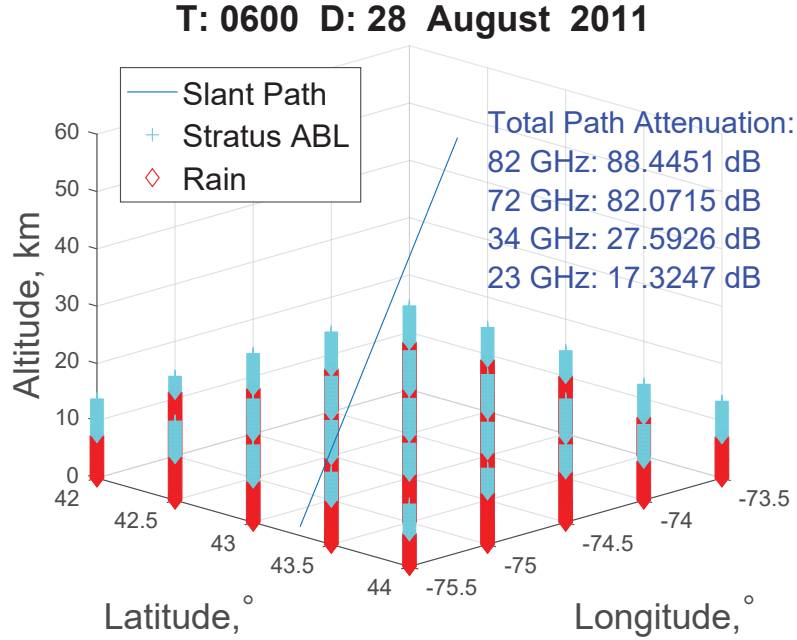


Figure 4.12: Worst case attenuation event with the most significant rainfall captured during the year using the five by five Weather Cube in trial four. The total path attenuation values due to aerosol, cloud, molecular, and rain effects are given.

by the ITU-R model. In particular the Weather Cube model over-estimates attenuation for almost all results. The error figure between the total path attenuation due to rain, compared against the ITU-R rain methodology and the total path attenuation due to clouds, compared to the ITU-R cloud methodology in trial two is given in Fig. 4.16. The error figure for the rain shows a large spike at the $p = 10\%$. The discontinuity in the error figure for rain is caused by the fact that the ITU-R rain model predicts 0 dB of rain attenuation above $p = 10\%$. This would force the error figure equation (Eq. 3.22) to become infinite, which by a visual inspection of Fig. 4.7 is not the case.

The inaccuracy of the rain model at these exceedance percentages may be caused by the fact that the Weather Cube weather placement algorithm only places liquid precipitation. While ice is generally present in all non-tropical regions, snow, freezing

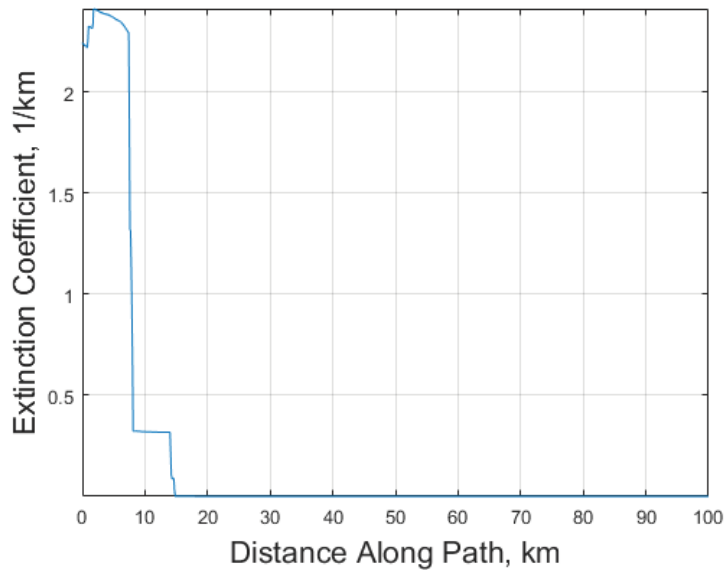


Figure 4.13: Extinction profile along the slant path for a worst case scenario attenuation event.

rain, and ice clouds are very likely to occur at the propagation path under consideration (Rome, NY). As the complex index of refraction of ice is less than that of liquid water, the attenuation incurred liquid precipitation is higher than that of frozen water. The assumption that all precipitation is liquid water can result in an over estimation of attenuation from rain. This is supported by the location of the maximum error ($p = 5$ to 15%) in each of the error figures, while at the lowest exceedance percentages ($p < 5\%$) the error figure is relatively low.

In analyzing the performance of the Weather Cube model for exceedance percentages less than $p < 5\%$, it is worth stating that the measured results for the two V and W band frequencies are only given for exceedance percentages greater than 0.9% . Without measured data for exceedance values less than 0.9% , a comparison is made with the total attenuation curve generated by the ITU-R total attenuation model given in Fig. 3.8. The largest source of attenuation for the lowest exceedance percentages is liquid rain. The ITU-

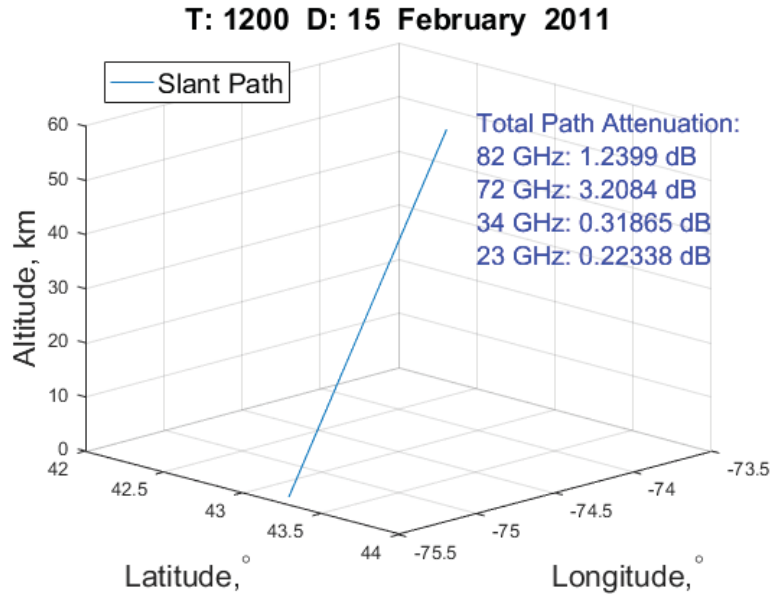


Figure 4.14: Least case attenuation event in which no rain or clouds were placed within the Weather Cube.

R model for rain attenuation predicts that the attenuation for 82 and 72 GHz should be in the range 40-50 dB at an exceedance probability of $p = 0.1\%$. The total attenuation values calculated by the Weather Cube model are much greater than that predicted by the ITU-R at the exceedance probability $p = 0.1\%$. The top four highest observed attenuation events for each frequency by the Weather Cube method are given in table 4.6. Whereas the ITU-R model for rain attenuation claims a validity for frequencies in the range 1-1000 GHz, several researchers have questioned the validity of ITU-R P.838 for use in EHF applications [39] [40]. Further research is needed to validate the attenuation values predicted by the Weather Cube for exceedance percentages less than $p < 5\%$.

Whereas the full five-by-five Weather Cube (trial four) appears to give more error than in the single profile case (trial two and three), the use of the full Weather Cube is still recommended. Improvements to the weather placement algorithm to include the effects of ice should give much lower error for the use of the full five by five case. When a

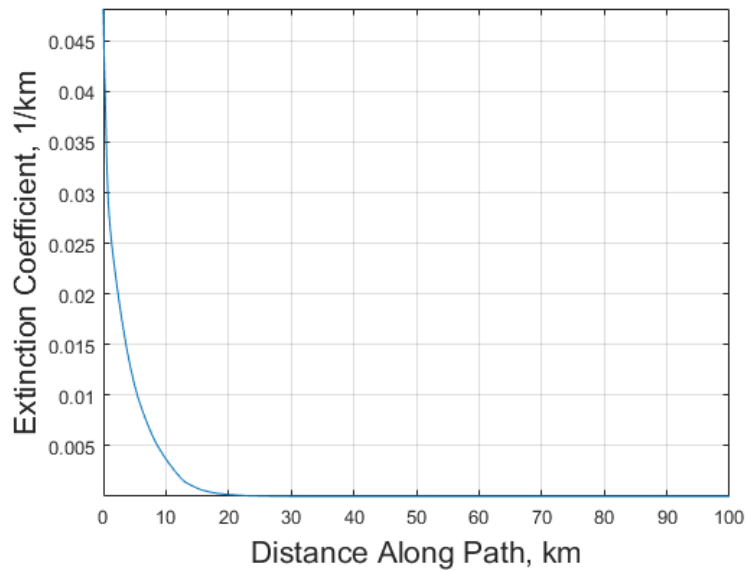


Figure 4.15: Extinction profile along the slant path for a least case attenuation event. Molecular extinction is the only effect calculated in this case. The extinction profile drops exponentially with altitude

single profile of weather data is used, only a single type of weather is placed for each weather observation resulting in a stair-case like shape of the exceedance curve as similar attenuation values are likely reported. Using the full five-by-five Weather Cube allows for weather diversity along the path, which results in much smoother attenuation curves.

Table 4.6: Highest Attenuation Values for Each Frequency from Trial Four

Order	Exceedance Percentage, %	82 GHz Attenuation, dB	72 GHz Attenuation, dB	34 GHz Attenuation, dB	23 GHz Attenuation, dB
1	0.0717	88.4451	82.0715	27.5926	17.3247
2	0.1435	56.9661	52.5624	15.8944	10.2606
3	0.2152	54.4466	50.6017	15.7726	10.1123
4	0.2869	54.0666	50.1253	15.5566	9.4939

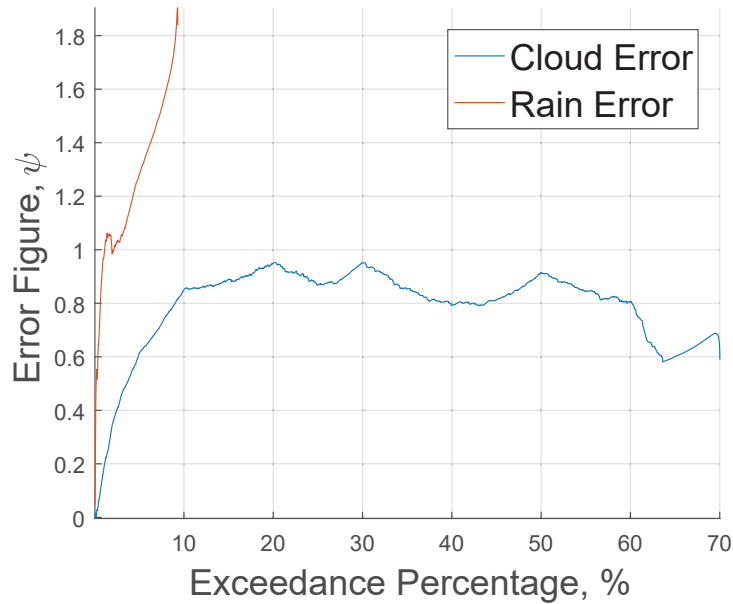


Figure 4.16: Error for rain and cloud effects from trial two. The error is defined as the error between the Weather Cube and ITU-R model derived exceedance curves. There is more error from the rain model as compared the the cloud model. There is an extreme peak of rain error at $p = 10\%$

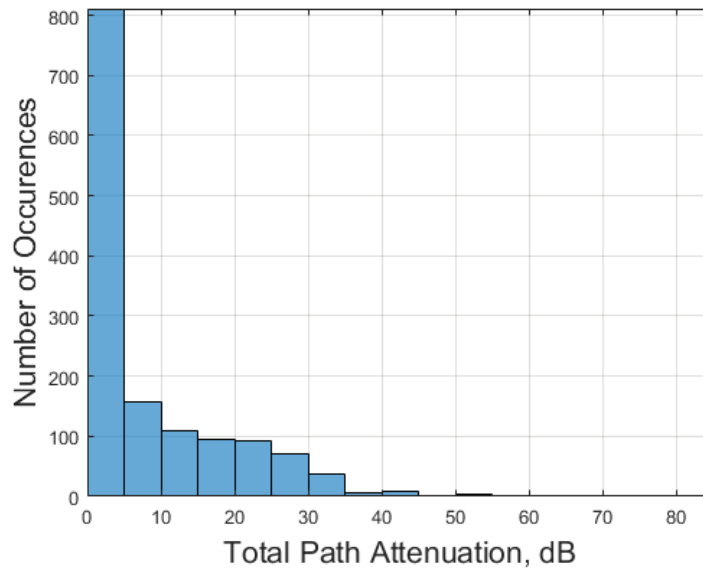


Figure 4.17: Histogram of total path attenuation values for 72 GHz from trial four.
Most of the 1,395 attenuation events observed were less than ten decibels.

V. Conclusion

5.1 Conclusion

In this study, the use of Weather Cubes compiled by the atmospheric characterization package LEEDR were used in an attempt to develop long-term attenuation statistics. While initial results show potential in this technique, further improvements to the weather placement algorithm must be made in order for this technique to be useful for any practical application. SATCOM links may require accurate exceedance data for as low as $p = 0.01\%$, therefore there is room for improvement with this methodology. As an initial evaluation of this methodology, this research provides several recommendations for improvement.

- The use of correlated-k or other band-averaged model should be used carefully in the V and W band, as the presence of several strong absorption lines gives very erroneous results.
- The calculation of total path attenuation currently employed in LEEDR can be made more accurate as compared to measurements not averaging the optical depth along the path (See Appendix A).
- The assumption that all precipitation is liquid water should be revisited. The inclusion of snow, ice, and freezing rain may increase the accuracy of the exceedance curves. The difference between liquid and solid water must be taken into account when using Mie Scattering to calculate precipitation extinction.

Additionally, this research provides a framework for future validation of long-term attenuation statistics derived from Weather Cubes against measured data.

5.2 Comparison With Other Models

In its present state, the Weather Cube methodology performs worse than the statistical NWP ITU-R model, and the instantaneous NWP model ATM PROP in terms of average error figure presented in [10]. There is no NWP based model that claims to be verified and validated. With the improvements or alternatives to the weather placement algorithm, it is expected that the Weather Cube methodology should reach a desired level of accuracy for practical use. The approach used in this research differs from those presented in [10] and [27]. In [27] a mesoscale model is used to give high resolution atmospheric characterization for the propagation path, while the Weather Cube methodology uses GFS with less resolution. Alternatively, [10] places inferred rain and cloud cells from a database of observed rain and cloud fields collected by a radar. In [10] not only are the presence of rains and clouds inferred, but also the spatial distribution. A study has not yet been performed on how fine of a resolution the atmospheric characterization data needs to be in order to calculate long-term attenuation statistics. Preliminary results reported in this thesis show that even with improvements needed in the weather placement algorithm, the exceedance curve can be partially captured using a single year of GFS data. The accuracy may be improved by simply using more years of available NWP data. The novel atmospheric characterization used in the Weather Cube may preclude the need for invoking more computationally expensive atmospheric models, which may be useful for the development of a global climatology study or for the development of empirical recommendations for engineering analysis. Additionally, the Weather Cube methodology does not rely on the accuracy of other models to calculate attenuation, as physics based extinction is calculated directly from Mie Scattering and by the line-by-line absorption method, albeit at the cost of higher-computational time for the attenuation calculations.

5.3 Application and Impact

Weather Cubes may eventually be used for two types of applications. The first is the long-term, climatology based attenuation studies similar to that presented in this research in which NWP data is pulled from databases for multiple years. This type of study may be useful in system development, or in the engineering development of PMT. A second potential application is in mission planning. The GFS data used allows ten day future forecast data. The Weather Cube methodology could be used to give decision makers a future expectation of system performance. This type of analysis can be applied to satellite communication or remote sensing applications.

5.4 Future Work

This research represents an initial attempt to use Weather Cubes to generate long-term attenuation statistics for RF earth-space links. Although initial results are promising, the Weather Cube methodology must be improved before verification and validation is performed.

5.4.1 Adjustment of Weather Placement Algorithm.

The disagreement between the Weather Cube derived exceedance curves and the radio sound derived curves at the lowest exceedance percentages is most likely due to limitations in the current weather placement algorithm. It is recommended that a study should undertaken to improve this algorithm. There are two issues with this algorithm that should be addressed. The first is the assumption that all precipitation throughout the year is liquid water. The index of refraction of snow and ice is different than that of liquid water, therefore the scattering and absorption from rain and clouds calculated using the current algorithm may be an over estimation. This effect can be significant in this research, as the path considered is modeled through the northern part of New York state, which is a region that typically encounters cold temperatures and snowfall. Additionally, the placement of the cloud field within a rain propagation shaft should be reconsidered. Currently a cloud is

placed from the middle of a cloud layer to the surface. It is suggested that this assumption be reconsidered, to attempt to create a more accurate cloud fields.

5.4.2 Verification and Validation.

Once the weather placement algorithm is adjusted, an attempt should be made to verify and validate the use of Weather Cubes in this application. Verification in this application means that the methodology generates similar results as those already used in this application. Validation refers to comparison with known truth data, to ensure the results are accurate. Full verification and validation cannot be performed at this time due to the lack of experimental data to compare against. In order to validate any methodology to generate long term path attenuation statistics, measured data is needed for a variety of geographic regions with varying climates. Comparisons between methodologies cannot be made by considering a single region of interest. The lack of experimental data also limits efforts for verification to similar comparison models, such as ATM PROP, that could potentially be used for verification, but cannot be validated. Validation can only be done as experimental research becomes available. There is an upper limit on how validated a methodology can be in this application.

This research was designed to demonstrate how verification and validation of Weather Cubes can be performed for a single location under study, with the expectation that a similar model will be used as more experimental data becomes available . In this thesis, the single slant path modeled was chosen to replicate the experiment performed by Brost and Cook in [8], so that the experimental data could be used in validation, while the ITU-R method developed in section 3.6 was used as verification data. The resulting performance metric of each methodology given in section 3.7 for a single location. A full comprehensive verification and validation can be done in the future by repeating this model process for any published experimental data, and then combining the individual performance metric from each study to give a combined score.

5.4.3 Tropospheric Scintillation.

The Weather Cube contains vertical profiles of the structure parameter for turbulence. It may be possible to use this data perform tropospheric scintillation studies, as measured data becomes available data with coherent phase information becomes available.

Appendix: Attenuation Calculations

A.1 Differences in Calculations

The calculation of total path attenuation differs from that currently used in LEEDR. In order to explain the differences between the two methodologies, and to provide justification as to why one is useful over the other, a derivation of both is given.

A.1.1 LEEDR Attenuation Methodology.

In LEEDR, the total path attenuation is not calculated directly. Instead a specific attenuation value for the entire length of the path is given. The total path attenuation can then be calculated by multiplying the specific attenuation by the entire path length. For a given vertical extinction profile β_e with N total extinction coefficients, LEEDR calculates a total path extinction E_{total} using

$$\Delta S = \frac{100}{N \sin(\theta)} \quad (A.1)$$

$$E_{total} = \frac{\sum_{n=1}^N \beta_e[n] \Delta S}{\sum_{n=1}^N \Delta S} \quad (A.2)$$

where ΔS is defined in Eq. 3.15. By multiplying the total path attenuation calculated by the attenuation constant ($10 \log_{10}(e)$), the specific attenuation in units of (dB/km) is calculated as

$$\gamma = 10 \log_{10}(e) E_{total}. \quad (A.3)$$

The total path attenuation in decibels is found multiplying the specific attenuation by the length of the slant path by

$$A_{dB} = \gamma \frac{100}{\sin(\theta)} \quad (A.4)$$

where the 100 is the LEEDR defined top of atmosphere, and θ is the elevation angle of the slant path. Further examination of Eq. A.2 yields,

$$E_{total} = \frac{\sum_{n=1}^N \beta_e[n] \Delta S}{\sum_{n=1}^N \Delta S} = \frac{\Delta S \sum_{n=1}^N \beta_e[n]}{\Delta S N} = \frac{1}{N} \sum_{n=1}^N \beta_e[n] \quad (A.5)$$

it is demonstrated that the total path extinction is the simple average extinction coefficient along the path. Although the forms of Eq. A.3 and Eq.3.3f are similar, A.3 calculates a specific attenuation γ in (dB/km), while Eq. 3.3f calculates a total integrated attenuation in A_{dB} .

The derivation of Eq. A.3, as it used in LEEDR, begins with the definition of specific attenuation. Using the equation for total attenuation. as defined in 3.3b, the specific attenuation for a slant path γ as

$$\gamma = \frac{10 \log_{10}(\frac{P_o}{P})}{L} = \frac{10 \log_{10}(e^{E_{total}L})}{L} \quad (A.7a)$$

where L is the total slant path length in km, and E_{total} is the total path extinction as defined in A.5. To simplify this equation, the logarithm change of base formula is used as

$$\log_{10}(X) = \frac{\ln(X)}{\ln(10)}. \quad (A.7b)$$

Applying the change of base formula to A.7a, the specific attenuation can be calculated as

$$\gamma = \frac{10}{L} \frac{\ln(e^{E_{total}L})}{\ln(10)} = \frac{10 E_{total} L}{L \ln(10)} = \frac{10}{\ln(10)} E_{total}. \quad (A.7c)$$

The constant $\frac{10}{\ln(10)} \approx 4.343$ is then the same number as the attenuation constant used in 3.3f.

There are two differences between the methodology currently employed in LEEDR.

A.1.2 Determination of Optical Depth .

Method one (currently used in LEEDR) calculates a total path attenuation by averaging the extinction coefficient along the slant path. This assumes that the optical depth of the atmosphere is evenly distributed throughout the entirety of the slant path. In general this is not a good assumption as the lower atmosphere tends to be more optically thick because of the presence of weather and because of the higher density of the atmosphere. This difference is especially detrimental with respect to cloud and rain events, which give relatively high extinction values over a small distance. Fig. A.1 gives a comparison of method one (M1) and method two (M2) for two frequencies, 82 GHz and 72 GHz, with

the radio sound data [8]. The results for M1 produce higher attenuation values than the expected measured data at all exceedance percentages, while M2 shows agreement for exceedance percentages above 55%.

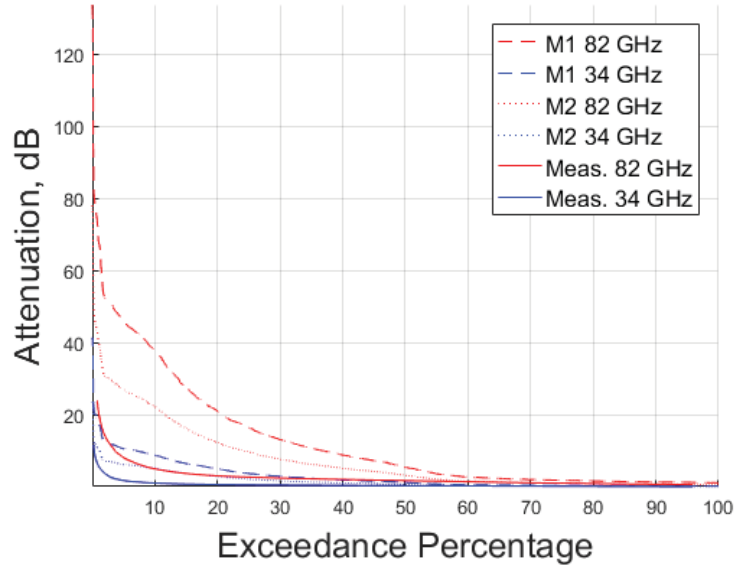


Figure A.1: Method One (The Method Currently Employed in LEEDR v. Method Two (The Method Used in this Work) [8].

A.1.3 Direction of Integration.

In method one the optical depth is calculated as the product of the slant path length ΔS , while in method two the optical depth is calculated as the product of the vertical component of the slant path ΔZ . As each extinction coefficient is calculated under the assumption of a horizontally stratified atmosphere, it is more natural for the vertical component to be used in the integral.

References

- [1] Schmidt, Jaclyn E. “4D Weather Cubes and Defense Applications”. *Defense Innovation Handbook*.
- [2] *ITU-R P.840-7 Attenuation due to clouds and fog*. Technical report, International Telecommunications Union (ITU-R), 2012.
- [3] Cianca, Ernestina, Tommaso Rossi, Asher Yahalom, Yosef Pinhasi, John Farserotu, and Claudio Sacchi. “EHF for satellite communications: The new broadband frontier”. *Proceedings of the IEEE*, 99(11):1858–1881, 2011. ISSN 00189219.
- [4] Fiorino, Steven T, Jarred Burley, Brannon J Elmore, Jaclyn E Schmidt, Elizabeth Matchefts, Cloud Fields, and Rain Fields. “Weather Cubes and 4D Visualizations Including Cloud and Rain Field Generated from Numerical Weather Prediction Data”. *33rd Conference on Environmental Information Processing Technologies*, 2017.
- [5] Marzano, Frank S., Luca Milani, Vinia Mattioli, Kevin M. Magde, and George A. Brost. “Retrieval of precipitation extinction using ground-based sun-tracking millimeter-wave radiometry”. *International Geoscience and Remote Sensing Symposium (IGARSS)*, 2016-Novem:2162–2165, 2016.
- [6] Mattioli, Vinia, Luca Milani, Kevin M. Magde, George A. Brost, and Frank S. Marzano. “Retrieval of Sun Brightness Temperature and Precipitating Cloud Extinction Using Ground-Based Sun-Tracking Microwave Radiometry”. *IEEE Journal of Selected Topics in Applied Earth Observations and Remote Sensing*, 10(7):3134–3147, 2016. ISSN 21511535.
- [7] Brost, G. and K. Magde. “On the use of the radiometer formula for atmospheric attenuation measurements at GHz frequencies”. *2016 10th European Conference on Antennas and Propagation, EuCAP 2016*, 2016.
- [8] Brost, George and Kevin Magde. “Ground-based radiometric measurements of slant-path attenuation in the V/W bands”. *Radio Science*, 49(12):1183–1193, 2014. ISSN 1944799X.
- [9] *ITU-R P.311-15 Acquisition , Presentation and Analysis of Data in Studies of Radiowave Propagation*. Technical report, International Telecommunications Union (ITU-R), 2015.
- [10] Luini, Lorenzo and Senior Member. “A Comprehensive Methodology to Assess Tropospheric Fade Affecting Earth Space Communication Systems”. 65(7):3654–3663, 2017.

- [11] Sklar, Bernard. *Digital Communications Fundamentals and Applications*. Prentice Hall PTR, Upper Saddle River, second edi edition, 2000.
- [12] Ippolito, Louis J. *Satellite Communications Systems Engineering: Atmospheric Effects, Satellite Link Design, and System Performance*. Wiley, West Sussex, 2008. ISBN 9780470725276 0470725273.
- [13] Petty, Grant. *A First Course in Atmospheric Radiation*. Sundog, Madison, 2004.
- [14] Sacchi, Claudio, Tommaso Rossi, Marina Ruggieri, and Fabrizio Granelli. "Efficient waveform design for high-bit-rate W-band satellite transmissions". *IEEE Transactions on Aerospace and Electronic Systems*, 47(2):974–995, 2011. ISSN 00189251.
- [15] De Sanctis, Mauro, Claudio Sacchi, Ernestina Cianca, and Tommaso Rossi. "Impulse-radio waveforms for MM-wave satellite communications: Potential benefits and open issues". *2016 10th European Conference on Antennas and Propagation, EuCAP 2016*, 2016.
- [16] Mulinde, Ronald, Talha Faizur Rahman, and Claudio Sacchi. "Constant-envelope SC-FDMA for nonlinear satellite channels". *GLOBECOM - IEEE Global Telecommunications Conference*, 2939–2944, 2013.
- [17] Rossi, Tommaso, Mauro De Sanctis, Fabio Maggio, Marina Ruggieri, Giuseppe Codispoti, and Giorgia Parca. "Analysis of Satellite Q/v band channel errors based on Italian experimental campaign". *IEEE Aerospace Conference Proceedings*, 1–9, 2017. ISSN 1095323X.
- [18] Crane, K. and W. Blood. *Handbook for the estimation of microwave propagation effects-link calculations for earth-space paths (Path Loss and Noise Estimation)*. Technical report, NASA Goddard Space Flight Center, Greenbelt, 1979.
- [19] Liebe, H.J. "An updated model for millimeter wave propagation in moist air". *Radio Science*, 20(5):1069–1089, 1985.
- [20] Murrell, David A., Steven A. Lane, Nicholas P. Tarasenko, and Christos Christodoulou. "A review of spaced based RF propagation experiments and examination of a new interest in W/V band (40-110 GHz) studies". *2016 IEEE Antennas and Propagation Society International Symposium, APSURSI 2016 - Proceedings*, 1527–1528, 2016.
- [21] Daoud, Nadine, Christos Christodoulou, Firas Ayoub, Nicholas Tarasenko, David Murrell, David Hensley, and Steven Lane. "Preliminary rain attenuation studies for W/V-band wave propagation experiment". *2016 USNC-URSI Radio Science Meeting (Joint with AP-S Symposium), USNC-URSI 2016 - Proceedings*, 113–114, 2016.
- [22] Nessel, James a, Roberto J Acosta, and Félix a Miranda. "Preliminary Experiments for the Assessment of V / W- band Links for Space-Earth Communications". 1616–1617, 2013.

- [23] *ITU-R P.618-13 Propagation data and prediction methods required for the design of Earth-space telecommunication systems*. Technical report, International Telecommunication Union (ITU-R), 2015.
- [24] Brost, G. A. and W. G. Cook. “Analysis of empirical rain attenuation models for satellite communications at Q to W band frequencies”. *Proceedings of 6th European Conference on Antennas and Propagation, EuCAP 2012*, (2):1455–1459, 2012.
- [25] *ITU-R P.838-3 Specific attenuation model for rain for use in prediction methods*. Technical report, International Telecommunications Union (ITU-R), 2005.
- [26] Luini, L. and C. Capsoni. “MultiEXCELL: A new rainfall model for the analysis of the millimetre wave propagation through the atmosphere”. *2009 3rd European Conference on Antennas and Propagation*, 1946–1950, 2009.
- [27] García, Maura Outeiral, Nicolas Jeannin, Laurent Féral, and Laurent Castanet. “Use of WRF Model to Characterize Propagation Effects in the Troposphere”. 1331–1335, 2013.
- [28] Fiorino, Steven T, Richard J Bartell, Matthew J Krizo, Kenneth P Moore, and Salvatore J Cusumano. “Validation of a worldwide physics-based, high spectral resolution atmospheric characterization and propagation package for UV to RF wavelengths”. *Proc. of SPIE*, 7090(709001), 2008.
- [29] Fiorino, Steven T., Robb M. Randall, Michelle F. Via, and Jarred L. Burley. “Validation of a UV-to-RF high-spectral-resolution atmospheric boundary layer characterization tool”. *Journal of Applied Meteorology and Climatology*, 53(1):136–156, 2014. ISSN 15588424.
- [30] Bohren, Craig and Donald Huffman. *Absorption and Scattering of Light by Small Particles*. Wiley-VCH Verlag GmbH & Co. KGaA, Weinheim, 2004.
- [31] *LEEDR Equations and Principles*. Technical report, AFIT Center For Directed Energy, 2017.
- [32] “HITRAN Online Database”, 2017. URL <http://hitran.org/about/>.
- [33] Wiscombe, W. J. “Improved Mie scattering algorithms”. *Applied Optics*, 19(9):1505, 1980. ISSN 0003-6935. URL <https://www.osapublishing.org/abstract.cfm?URI=ao-19-9-1505>.
- [34] *ITU-R P.676-11 Attenuation by atmospheric gases*. Technical report, International Telecommunications Union (ITU-R), 2016.
- [35] *ITU-R P.835-5 Reference standard atmospheres*. Technical report, International Telecommunications Union (ITU-R), 2012.

- [36] *ITU-R P.839-4 Rain Height Model for Prediction Methods*. Technical report, International Telecommunications Union (ITU-R), 2013.
- [37] *ITU-R P.1511-1 Topography for Earth-space propagation modelling*. Technical report, International Telecommunications Union (ITU-R), 2015.
- [38] *ITU-R P.837-7 Characteristics of precipitation for propagation modelling*. Technical report, International Telecommunication Union (ITU-R), 2012.
- [39] Kim, Jong Ho, Myoung Won Jung, Young Keun Yoon, and Young Jun Chong. “The measurements of rain attenuation for terrestrial link at millimeter Wave”. *International Conference on ICT Convergence*, 848–849, 2013. ISSN 21621241.
- [40] Hong, Eugene, Steven Lane, David Murrell, Nicholas Tarasenko, and Christos Christodoulou. “Terrestrial link rain attenuation measurements at 84 GHz”. *2017 United States National Committee of URSI National Radio Science Meeting, USNC-URSI NRSM 2017*, 2016:3–4, 2017.

REPORT DOCUMENTATION PAGE					Form Approved OMB No. 0704-0188	
<p>The public reporting burden for this collection of information is estimated to average 1 hour per response, including the time for reviewing instructions, searching existing data sources, gathering and maintaining the data needed, and completing and reviewing the collection of information. Send comments regarding this burden estimate or any other aspect of this collection of information, including suggestions for reducing the burden, to Department of Defense, Washington Headquarters Services, Directorate for Information Operations and Reports (0704-0188), 1215 Jefferson Davis Highway, Suite 1204, Arlington, VA 22202-4302. Respondents should be aware that notwithstanding any other provision of law, no person shall be subject to any penalty for failing to comply with a collection of information if it does not display a currently valid OMB control number.</p> <p>PLEASE DO NOT RETURN YOUR FORM TO THE ABOVE ADDRESS.</p>						
1. REPORT DATE (DD-MM-YYYY) 22-03-2018		2. REPORT TYPE Master's Thesis		3. DATES COVERED (From - To) August 2016 - March 2018		
4. TITLE AND SUBTITLE Satellite Communications in the V and W Band: Tropospheric Effects				5a. CONTRACT NUMBER		
				5b. GRANT NUMBER		
				5c. PROGRAM ELEMENT NUMBER		
				5d. PROJECT NUMBER JON 18G207		
6. AUTHOR(S) Shelters, Bertus A, 2d Lt				5e. TASK NUMBER		
				5f. WORK UNIT NUMBER		
7. PERFORMING ORGANIZATION NAME(S) AND ADDRESS(ES) Air Force Institute of Technology Graduate School of Engineering and Management (AFIT/EN) 2950 Hobson Way Wright-Patterson AFB OH 45433-7765				8. PERFORMING ORGANIZATION REPORT NUMBER AFIT-ENG-18-M-060		
9. SPONSORING/MONITORING AGENCY NAME(S) AND ADDRESS(ES) Air Force Research Laboratory: Information Directorate 26 Electronic Parkway Rome, NY 13441-4514 DSN 587-7418, COMM 315-330-4409 Email: paul.gilgallon@us.af.mil				10. SPONSOR/MONITOR'S ACRONYM(S) AFRL/RITF		
				11. SPONSOR/MONITOR'S REPORT NUMBER(S)		
12. DISTRIBUTION/AVAILABILITY STATEMENT DISTRIBUTION STATEMENT A: APPROVED FOR PUBLIC RELEASE; DISTRIBUTION UNLIMITED.						
13. SUPPLEMENTARY NOTES This work is declared a work of the U.S. Government and is not subject to copyright protection in the United States.						
14. ABSTRACT An investigation into the use of Weather Cubes compiled by the atmospheric characterization package, Laser Environmental Effects Definition and Reference (LEEDR), to develop accurate, long-term attenuation statistics for link-budget analysis is presented. A Weather Cube is a three-dimensional mesh of numerical weather prediction (NWP) data plus LEEDR calculations that allows for the quantification of rain, cloud, aerosol, and molecular effects at any UV to RF wavelength on any path contained within the cube. The development of this methodology is motivated by the potential use of V (40-75 GHz) and W (75-110 GHz) band frequencies for the satellite communication application, as V and W band frequencies incur very significant lower atmospheric attenuation. Total path attenuation probability of exceedance curves are compared against ground based radiometric measurements of slant-path attenuation in the V and W bands, as well as relevant International Telecommunication Union recommendations. The results of this work demonstrate the need for further improvements in this methodology.						
15. SUBJECT TERMS V Band, W band, EHF, Atmospheric Propagation						
16. SECURITY CLASSIFICATION OF:			17. LIMITATION OF ABSTRACT	18. NUMBER OF PAGES	19a. NAME OF RESPONSIBLE PERSON Dr. Andrew J. Terzuoli, AFIT/ENG	
a. REPORT	b. ABSTRACT	c. THIS PAGE			19b. TELEPHONE NUMBER (Include area code) (937) 785-3636 x4717 Andrew.Terzuoli@afit.edu	
U	U	U	UU	84		